Marta Cristina Bravo de Moreira Pinto

Bachelor Degree in Biomedical Engineering Sciences

Validity of 4DCT determined internal target volumes in radiotherapy for free breathing lung cancer patients

Dissertation submitted in partial fulfillment
of the requirements for the degree of

Master of Science in
Biomedical Engineering

Adviser: Kenneth Wikström, Medical Physicist, Uppsala University Hospital

Co-adviser: Pedro Vieira, Associate Professor, Faculty of Sciences and Technology, NOVA University of Lisbon

Examination Committee

Chairperson: Doctor Carla Maria Quintão Pereira
Raporteur: Doctor João Duarte Neves Cruz
Member: Doctor Pedro Manuel Cardoso Vieira

FACULDADE DE CIÊNCIAS E TECNOLOGIA
UNIVERSIDADE NOVA DE LISBOA

November, 2017

Validity of 4DCT determined internal target volumes in radiotherapy for free breathing lung cancer patients

Copyright © Marta Cristina Bravo de Moreira Pinto, Faculty of Sciences and Technology, NOVA University of Lisbon.

The Faculty of Sciences and Technology and the NOVA University of Lisbon have the right, perpetual and without geographical boundaries, to file and publish this dissertation through printed copies reproduced on paper or on digital form, or by any other means known or that may be invented, and to disseminate through scientific repositories and admit its copying and distribution for non-commercial, educational or research purposes, as long as credit is given to the author and editor.

This document was created using the (pdf)LaTeX processor, based in the "unlthesis" template[1], developed at the Dep. Informática of FCT-NOVA [2].
[1] https://github.com/joaomlourenco/unlthesis [2] http://www.di.fct.unl.pt

To my family and friends, who were always there for me

Acknowledgements

I would like to start by acknowledge the support, guidance and dedication of my supervisor Kenneth Wikström through the development of this thesis work in the six months I was in Sweden, and even after that. His skills and knowledge showed me a new field of research with undoubtedly interest for me. In addiction to this, I also got the chance to get to know the Swedish culture in a closer way through his stories and interesting facts. Thank you!

I am also thankful to professor Anders Ahnesjö for accepting me in his inspiring research group and to David Boersma for giving me the opportunity to have an interesting project to work in and for his encouragement and delightful jokes. I would also like to thank Samuel Fransson and Tufve Nyholm for their availability to introduce me to MICE software for my thesis work. In addiction, I extend my gratefulness to Uppsala University which was my host university in Sweden.

To all the remaining members of the research group I was in, namely Fernanda Navarro, Erik Almhagen, Eric Grönlund, David Tilly, and to all the medical physicists I talked to, thank you for making me feel welcome, for all the good moments and fika times, as well as for all the interesting lunch discussions about everything.

To FCT-UNL, my home university, and all the professors who made part of my path in the past 5 years, I am sincerely thankful for all the knowledge you gave me which contributed for this thesis development. Particularly, to professor Pedro Vieira for his time and patience to answer all my questions and for his guidance and help through my thesis progress.

Finally, I would like to acknowledge my family and friends for the motivation they gave through this work and through university. Specially my father, who always told me to "keep it simple", either in my studies and work or in my life, my mother, for being the positive person I needed most of the times in my stressful periods, and my sister, for always telling me to stop being lazy and go to work (thank you sis). I would like to mention the support and attentiveness of my grandparents through my college period and I want to thank you for always checking on me.

Abstract

Background: With both high incidence and death rate, lung cancer accounts for a large burden of disease worldwide. In many cases, these patients receive radiotherapy. Commonly, margins are added to the treatment volume to avoid underdosage due to the respiration-induced tumour motion. Four-Dimensional Computer Tomography (4DCT) is an imaging technique that is capable of capturing the lung tumours as they move during respiration, which enables the creation of individualized margins. However, the technique requires regular breathing during the entire scan to avoid breathing motion artefacts. Many patients do not fulfil this requirement. Moreover, there is also a substantial risk of encountering irregularities in the breathing pattern during the 4-8 minutes that are usually needed for treatment delivery. Hence, there is a potential risk of underestimating the tumour volume and its motion, i.e., the Internal Target Volume (ITV), for patients with irregular breathing patterns. We aim to investigate the risk of underestimating a 4DCT determined ITV due to irregular breathing patterns during a typical treatment period.

Method: For 5 patients, the ITV was extracted from a 4DCT scan and compared to the ITV extracted in the sum of 150 cine images (3 x 50). The cine images were acquired during 4 minutes in three different sessions. All ITVs were obtained through segmentation.

Results: It was found that ITVs obtained from the 4DCT scan were smaller than the ones from the cine images case, and the statistical analysis done confirmed this at a significance level of 5%.

Conclusion: We conclude that the required margin to handle respiratory-induced tumour motion can be underestimated for patients with irregular breathing pattern if the ITV is based on a conventional treatment planning 4DCT. The main cause for this is inter-fractional variations.

Keywords: 4DCT, Non-Small Cell Lung Cancer, Radiotherapy, Irregular Breathing, ITV

Resumo

Contexto: O cancro do pulmão apresenta elevadas taxas de incidência e mortalidade em todo o mundo. Pacientes com esta condição recebem frequentemente tratamento por radioterapia. Nestes casos, são adicionadas margens ao volume a ser tratado para evitar subdosagem devido a movimentos tumorais decorrentes da respiração. A Tomografia Computorizada a Quatro Dimensões (4DCT, sigla inglesa) é uma técnica de imagem capaz de capturar o tumor durante o movimento de respiração, permitindo a criação de margens individualizadas. No entanto, a técnica requer uma respiração regular durante toda a aquisição, por forma a evitar artefactos nas imagens. Muitos dos pacientes não cumprem este requisito, existindo o risco adicional de se encontrarem também irregularidades na respiração durante os 4-8 minutos que são normalmente utilizados para tratamento. Consequentemente, poder-se-á subestimar o volume do tumor e o seu movimento, i.e., o Volume do Alvo Interno (ITV, sigla inglesa), para pacientes com respiração irregular. Assim, este estudo tem como objetivo investigar o risco de se subestimar o ITV determinado por uma 4DCT devido à respiração irregular presente durante o tratamento.

Método: O ITV extraído de um scan de 4DCT foi comparado com o extraído da soma de 150 imagens cine (3 x 50), em 5 pacientes. As imagens cine foram adquiridas durante 4 minutos em três sessões diferentes. Todos os ITVs obtidos foram extraídos através de segmentação.

Resultados: ITVs produzidos num scan de 4DCT apresentaram volumes menores face aos ITVs obtido por imagens cine, tendo esta observação sido confirmada através da análise estatística feita para um nível de significância de 5%.

Conclusão: Concluiu-se que a margem necessária para incluir movimentos tumorais decorrentes da respiração poderá ser subestimada para pacientes com respiração irregular, caso o ITV seja baseado num plano de tratamento convencional de 4DCT. A causa principal deve-se a variações na respiração entre sessões de tratamento.

Palavras-chave: 4DCT, Cancro do Pulmão de Não Pequenas Células, Radioterapia, Respiração Irregular, ITV

Contents

List of Figures

List of Tables

Acronyms

3DCT	Three-Dimensional Computed Tomography.
4DCT	Four-Dimensional Computed Tomography.
CBCT	Cone-Beam Computed Tomography.
CT	Computed Tomography.
CTV	Clinical Target Volume.
DICOM	Digital Imaging and Communications in Medicine.
dMRI	Dynamic Magnetic Resonance Imaging.
DSC	Dice's similarity coefficient.
GTV	Gross Tumour Volume.
ICRU	International Commission on Radiation Units and Measurements.
IGTV	Internal Gross Target Volume.
ITK	Insight Segmentation and Registration Toolkit.
ITV	Internal Target Volume.
MICE	Medical Interactive Creative Environment.
MIP	Maximum Intensity Projection.

NSCLC	Non-Small Cell Lung Cancer.
PET	Positron Emission Tomography.
PTV	Planning Target Volume.
SBRT	Stereotactic Body Radiation Therapy.
SCLC	Small-Cell Lung Cancer.
WHO	World Health Organization.

Chapter 1

Introduction

1.1 Motivation

Motion information during image acquisition is of great importance when dealing with lung cancer patients. In many cases, these patients are receiving radiotherapy, where target (tumour) position and its displacements from a reference position are of great importance as we only want to deliver radiation to the necessary volume [1]–[3]. In order to do that, a treatment plan has to be designed [4]. These treatment plans take into account the tumour volume, tumour motion and patient setup errors [2], [5]. Commonly, a Four-Dimensional Computed Tomography (4DCT) scan is used for treatment planning since it creates Computed Tomography (CT) images with fewer motion artefacts associated [2], [4], [6], [7] compared to a non-respiratory correlated Three-Dimensional Computed Tomography (3DCT) scan [3], [6], [7]. By using an external respiratory surrogate to acquire the breathing trace simultaneously to the image acquisition and reconstruct the tumour volume based on that information, the use of 4DCT images avoids possible motion artefacts [2]. This way, it is possible to access the tumour volume, create an individual treatment plan and deliver a high dose to the tumour whilst keeping the dose to the surrounding normal tissue as low as possible.

Nevertheless, the scan obtained from the 4DCT technique is acquired during a maximum of two breathing cycles per voxel and hence, limited motion information is gathered in the CT data sets obtained. Therefore, in the case of irregular breathing patients, the risk of encountering non-predicted tumour motions [8] during several minutes of treatment delivery can thereby be considerably large. So, even though 4DCT is a good method to reduce the motion artefacts, it still requires a regular breathing pattern, i.e., constant frequency and amplitude. As a result, when dealing with patients with irregular breathing pattern, the validity of the treatment plan created based on a 4DCT is compromised

[9], [10].

The present thesis emerges as an effort to assess whether the 4DCT scans can indeed affect the volumes used to create the treatment plan, in the case of patients with irregular breathing pattern.

1.2 Thesis Objective

The main problem approached by this thesis's work is related to the uncertainties associated with the Internal Target Volume (ITV) obtained from a 4DCT scan acquired from patients with an irregular breathing pattern.

Commonly, lung cancer radiation treatment plans are based on images obtained from 4DCT scans, as a way to obtain tumour motion with less image artefacts associated. However, the limited scan time, together with an irregular breathing pattern, gives a high risk of getting a tumour motion (i.e., an ITV) associated only with a certain part of the respiratory trace. This may not match the tumour motion during treatment delivery, particularly since the treatment delivery is based on a 4DCT scan done several days or weeks before treatment. Besides, irregular breathing patterns might also lead to other types of image artefacts and hence incorrect definition and delineation of tumour volume.

In this sense, the aim is to give an estimative of the risk of missing (underdosing) the target (tumour) in radiotherapy planned on a 4DCT acquired during free breathing. More specifically, the goal can be specified by the following questions:

1. Is the ITV value different when a 4DCT scan is used to obtain it?

2. Can we identify the factors that influence the ITV construction?

To answer these questions, the following methodology is going to be used: a conventional 4DCT scan with 10 breathing phases will be compared to a different image acquisition method proposed for this study, in which 3DCT scans are acquired in cine mode at random times.

The aim is to calculate the needed margins to cover both the tumour volume and its motion (i.e., the ITV) in both sets of images. To accomplish this, an algorithm is going to be developed in order to semi-automatically segment the tumour from each set of images and add the margins needed to account for the ITV.

It is assumed that the scans acquired at random times will create a better estimate of the tumour motion compared to the 10 phases determined in the 4DCT data set. Hence, the 3DCT data set would give a more representative ITV.

Based on this assumption, if the ITV extracted from the 4DCT data set differs from the one obtained in the 3DCT data set, then the ITV obtained from the 4DCT is not being correctly defined. Therefore, if the ITV from a 4DCT scan is smaller than the ITV

from the 3DCT method, then there is a risk of underdosing the tumour during treatment delivery.

It should be noted that this work only handled geometrical issues, hence, no dosimetric evaluation was done.

By finding the adequate software to support this methodology, which accesses and extracts the ITVs obtained from the two acquisition methods, the algorithm will be developed and a comparison between the acquisition methods will be accomplished. This way the thesis's first question will be analysed, whereas the second question can be answered through the process of literature reading together with actual ITV construction steps interpretation, i.e., through the observation and proposal of potential influencing factors in the ITV construction.

1.3 Research Context

The research described in this thesis was done within a research group in Medical Radiation Physics, from the Department of Immunology, Genetics and Pathology at Uppsala University Hospital, Sweden. Nevertheless, its development had also the support from Faculty of Sciences and Technology and the NOVA University of Lisbon, Portugal.

1.4 Contribution

The present work will provide a novel approach to directly assess 4DCT's scans and obtain the ITVs as well as to identify influencing factors to the ITV construction. It will also constitute a base for further improvements, e.g. added surrogate information, in order to increase the robustness and validity of the treatment plans.

1.5 Thesis Outline

This thesis is organized in six chapters. Starting with the present one, were a brief description of the motivation, goal, research context and contribution of the thesis is done, the following ones are:

Chapter 2 which introduces the basic concepts behind the technique used.

Chapter 3 where a literature review is presented. In other words, this chapter reveals the relevance the study has in its field of research.

Chapter 4 which is about the patients studied and the methodology used.

Chapter 5 where the results obtained in this work are presented and discussed.

Chapter 6 is the final chapter and it presents the general conclusions taken from this work, this study limitations, as well as future work perspectives for further researches regarding the 4DCT usage in lung cancer patients' treatments.

Chapter 2

Background

The present chapter describes the concepts that are relevant to understand the thesis and its context. This includes the medical context in which the technique used (i.e., the 4DCT) is being addressed, why it is normally used, how it is used and how it works, what are its limitations as well as what affects its normal use.

2.1 Medical Context

With approximately 14 million new cases and 8 million deaths in 2012, cancer figures among the leading causes of morbidity and mortality worldwide, according to a publication made by the *World Health Organization (WHO)* [11].

2.1.1 Lung Cancer

In that same publication, the WHO shows that lung cancer accounts for a large burden of disease worldwide, with more than 1.8 million new cases (13% of total cancer incidence) diagnosed in 2012 and almost 1.6 million deaths (20% of total cancer mortality), being also regarded as the fourth most common type of cancer in Europe.

Lung cancer is described as one of the most aggressive human cancers, with a survival rate of 10–15% after 5-years, and for men it is the most common cancer-related death, while in women it appears as the third most usual cause, also according to the WHO report.

This type of cancer can be classified according to two major histological subtypes: Small-Cell Lung Cancer (SCLC) and Non-Small Cell Lung Cancer (NSCLC), the latter representing 85% of all cases [12]–[14]. In this master's thesis, all of the patients recruited for the study were diagnosed with NSCLC.

Regarding the treatment given to lung cancer patients, it can include options such as radiotherapy, surgery and chemotherapy [14], [15]. However, the use of chemotherapy and surgery options is somehow limited. Surgery is not normally performed due to issues as age and co-morbidities in the patients being treated, while chemotherapy treatment is related to high toxicities and low improvement in local control [14], [16]. Therefore, radiotherapy can be considered "a principal treatment modality for unresectable lung tumors and is also used in combination with surgery or chemotherapy" [16, p. 158]. In the present work, this latter type of treatment was the one applied to the NSCLC patients.

2.1.2 Radiotherapy

Radiotherapy, or Radiation Therapy, attempts to kill tumour cells by using ionizing radiation. The main goal is to damage the DNA of this cancer cells while sparing normal tissue. To accomplish that, the radiation is delivered to the patient in fractions in a process called *fractionation of dose* [17, Ch. 13, p. 440]. Dose is defined as the energy absorbed per unit mass at a certain point. What fractionation means, is that this energy is given to the tissue over a certain period of time (e.g weeks), instead of all at once. If the fractioning is used with adequate times between applications, then this process allows normal cells to recover, while tumour cells are less efficient repairing their damage.

In addition, this work will be dealing with external beam radiotherapy which means that the treatment is applied from outside of the body and that all the tissue in the path of the beam will receive some radiation dose. So, using techniques like Three Dimensional Conformal Radiotherapy, Stereotactic Radiotherapy (also known as Stereotactic Body Radiation Therapy (SBRT)), Image Guided Radiotherapy and Intensity Modulated Radiotherapy [15], [18], will also help to preserve the normal tissue and organs at risk (e.g. the heart) by exactly determining where the tumour is and shape the high dose region closely around the tumour volume.

CT images alone, or in combination with Positron Emission Tomography (PET) [19], [20], are acquired prior to the treatment to image the patient in the treatment position. Based on these CT images and with the help of a computer software, the treatment plan can be created and the treatment delivery optimized. The primary goal of this plan is to cover the tumour volume with high dose while sparing as much as possible the normal tissue.

The treatment plan, which includes the CT images with a set of delineated target volumes, is then transferred to the treatment machine and the machine delivers the treatment plan [4, Ch. 12, pp. 170-181].

2.1.3 Respiratory Motion in Radiotherapy

Nowadays, radiotherapy treatments are very accurate in delivering high dose radiation to the region of interest, but, to be efficient, the tumour position is required. Therefore, it is important to notice that respiratory motion must be considered in lung cancer patients

as the breathing movement changes the tumour position and consequently affects proper tumour targeting [19].

Under these circumstances, respiratory motion margins must be added to the delineated target (tumour) volume, in order not to miss it during treatment. These added margins generate different volumes which, as they will be described in section 2.2.4, are used to cover the target volume as well as to include the large and variable motion from the tumour. Furthermore, in order to identify and track tumour's position and respective motion, good imaging methods are also needed.

It has already been reported in some articles how the tumour moves in the lung, providing a general idea of what to expect during image acquisition and treatment delivery. For example, Liu *et al.* study showed that the main direction taken by the tumour motion was craniocaudal, which was in line with previous studies, and that this motion is also highly correlated to the diaphragm motion [1]. It was also mentioned in the study that the treatment margins should be anisotropic, so that tumour motion in the three dimensions was taken into account. Finally, in the same study, Liu *et al.* mentioned that the "magnitude of tumour motion is likely dependent on not only patient factors (e.g., regularity of breathing) but also tumour-related factors (e.g., location and size)" [1, p. 532], which demonstrates how complex and highly patient dependent the motion of lung tumours can be.

2.2 Image Acquisition

It was made clear that there is a need to find an adequate imaging method that allows to see the extent of tumour motion in the lungs. As reported from Keall *et al.* [2], there are various methods to image organ motion, like Ultra-Sound, CT, Magnetic Resonance, Nuclear Medicine and Fluoroscopy.

As CT scanners' images are known to historically provide basic information to define treatment volumes as well as information on electron density, which enables the calculation of three dimensional radiation dose-distribution, these equipments are commonly used for treatment planning [20, p. 1]. Besides, they constitute essential equipments in all well-equipped radiation oncology departments, which also made them one of the main methods used for treatment planning.

2.2.1 Computed Tomography Imaging

In CT scans an x-ray source is rotated around the patient with about 2 revolutions per second (see Figure 2.1). A detector array detects the photons that are passing through the patient and by means of reconstruction algorithms, a 3DCT image can be reconstructed. CT has become a high contrast imaging modality that distinguishes itself from conventional radiography for allowing the display of anatomy across planes (e.g. axial

or transverse, coronal and sagittal sections), which is very useful for visualizing distinct anatomical parts of the human body [4, Ch. 11, pp. 154-169].

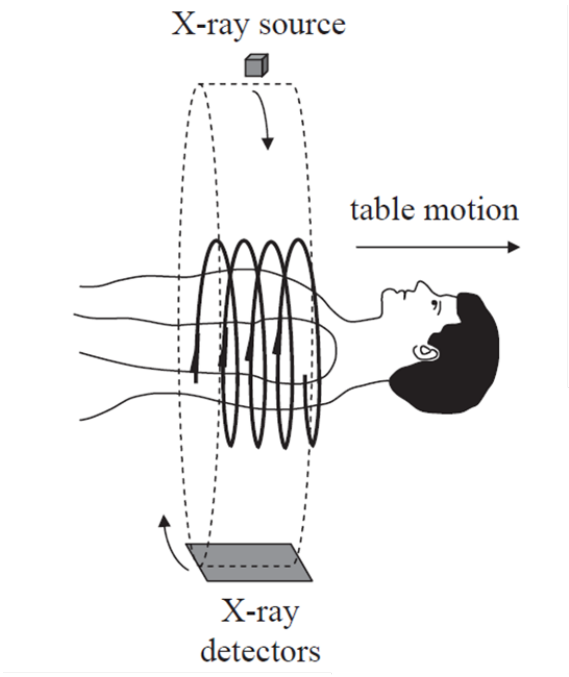

Figure 2.1: Example of a CT scan in helical mode with representation of the x-ray source and detectors movement, as well as the table motion direction. (Adapted from [21, Ch.2, p. 67])

In radiotherapy, CT images are commonly reconstructed as a set of two dimensional axial slice images of the patient at given couch positions, with slice widths that normally are 1.5-3mm, but can potentially be from 0.4mm to 1cm. The use of the successive slices enables the extraction of the corresponding volume elements (voxels) of tissue in the patient. By combining these voxels mathematically, it is possible to obtain coronal and sagittal images, which are currently used in CT imaging routine [4, Ch. 11, pp. 154-169].

2.2.2 Respiratory Motion in Image Acquisition

As it has been mentioned before in section 2.1.3, the main direction of motion by tumours in the lung is craniocaudal. Since this is the same direction of motion as the CT couch (see Figure 2.1), the volume of the body being imaged is going to move in and out of the CT slice window while the scanning process of a specific slice is being done [4, Ch. 12, pp. 170-181]. Hence, motion artefacts will be created in the CT image (see Figure 2.2) which will then conflict with target delineation, a crucial step in the radiotherapy treatment, and dose calculation [4, Ch. 12, pp. 170-181].

Besides, if the time needed to acquire a CT data set is not shorter than a respiratory cycle, then a certain portion of the body that is constantly moving will be imaged. This is what actually happens, since a normal respiratory period has approximately the same

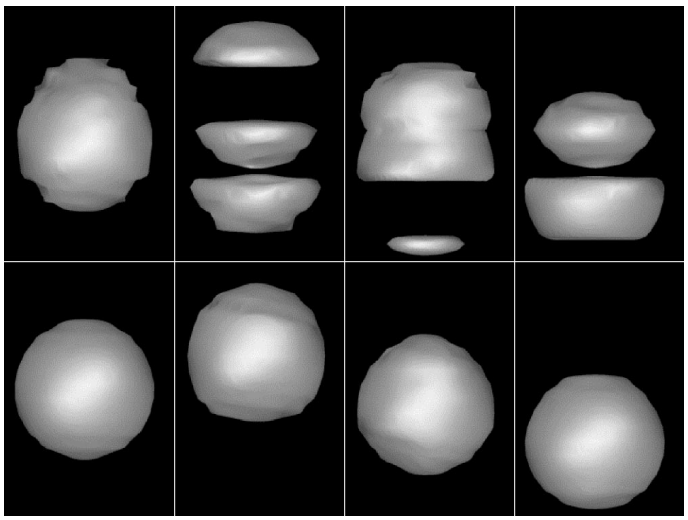

Figure 2.2: Images of a spherical object CT scanned during periodic motion simulated respiration. Artefacts created by this periodic motion incorrectly characterize the geometric shape and extent of an organ when no breathing information is presented (top images). When the sphere is imaged using other image modalities (like 4DCT, explained further on), the motion artefacts can be reduced (bottom images). (Adapted from Rietzel *et al.* [6])

time needed to acquire a CT data set [4, Ch. 12, pp. 170-181], and this is also why motion artefacts will be present in the final image.

Nevertheless, Keall *et al.* [2] showed that there are methods to reduce the impact of respiratory motion in radiotherapy, like the motion-encompassing methods. These methods include three techniques for CT imaging, capable of giving access to the entire range of tumour motion, in a certain breathing period. They are the Slow CT, the Inhalation and Exhalation Breath-Hold CT, and the Respiration-Correlated or 4DCT. The main interest in this project is to evaluate the 4DCT validity and so in the next section this technique will be described.

2.2.3 Four-Dimensional Computed Tomography (4DCT)

As a fine solution to obtain high quality CT data in the presence of respiratory motion, 4DCT is a good choice when dealing with treatment planning and delivery to lung cancer patients [2]. The main reason for this is the fact that this type of imaging technique uses real-time recording of a respiratory signal while doing image acquisition.

By imaging the same anatomy several times at different respiratory phases during a large number of breathing cycles, an oversampling of CT images is acquired. Through the use of the respiratory signal recorded simultaneously, the acquired images can be tagged to a specific respiratory phase, as we can see in Figure 2.3. As a result, several 3DCT image data sets can be sorted into bins according to the tagged phase information [22, Ch. 1, pp. 4-7]. Therefore, a 4DCT method, as reported by Hutchinson and Bridge , is essentially formed by "an oversampled 3DCT scan, which can be separated into phases

of the breathing cycle to determine time-specific target positions" [14, p. 71].

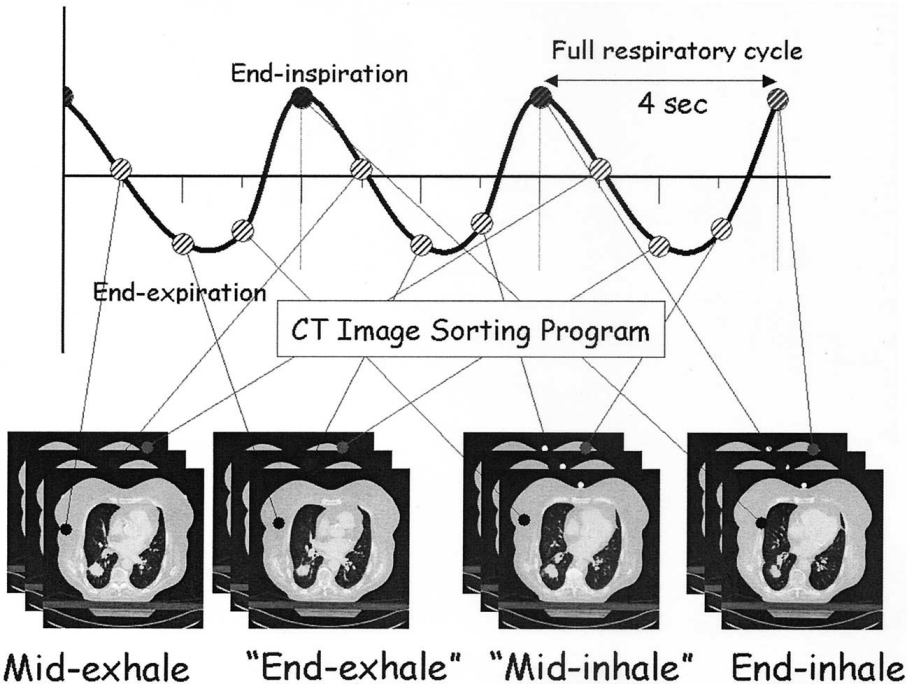

Figure 2.3: Respiratory sorting of CT images from a 4DCT data set, according to a breathing phase, and respective binning. (Adapted from Underberg *et al.* [23])

The algorithm used for the sorting, and consequent binning process, can be implemented through *phase binning* or *amplitude binning* (see Figure 2.4). In the phase binning process, the acquired CT images are sorted according to phase. Phase is defined as the fraction of elapsed time since last peak of the breathing trace in relation to the cycle time (peak-to-peak time). This means that phase binning is time based [24]. In amplitude binning, the acquired CT images are simply sorted according to the amplitude of the respiratory signal. If the a certain amplitude level is missing for some CT images due to irregularities in the breathing pattern, the algorithm chooses the images with amplitude as close as possible (see Figure 2.4, second 50% bin point from the amplitude binning image) [24].

Regarding the data acquisition by this technique, it can be accomplished in two ways: *prospective* and *retrospective* gating. In the first case, the image acquisition is triggered by events in the respiratory trace, such as transitions from an inspiration point to expiration, for example. In the second case, images are acquired during all phases of the respiratory cycle and after the data acquisition has ended, a software then correlates the acquisition time of the images to the desired phase of the respiratory cycle, by using the respiratory signal that was recorded simultaneously with the image acquisition [25].

In a 4DCT scan, data can be acquired in a *helical mode*, where the table the patient is lying on moves slowly and continuously to allow acquisition of data in closely spaced slices; or in an *axial cine mode*, where the table is fixed in a certain position and the

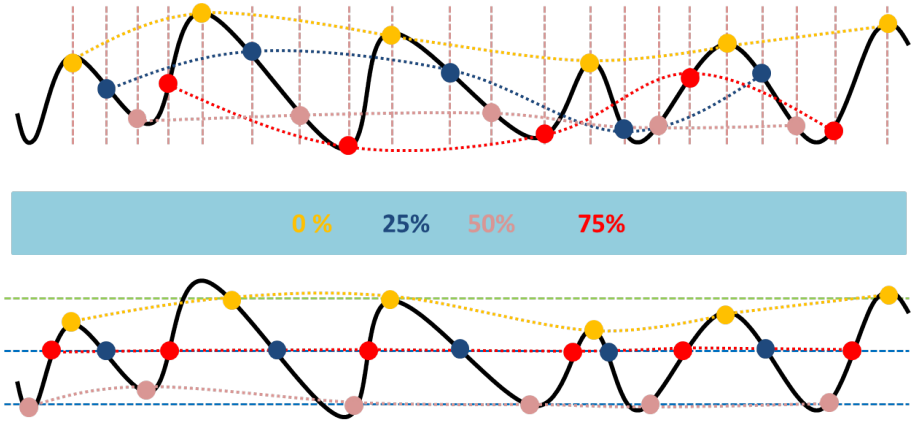

Figure 2.4: Sorting process for an irregular breathing waveform, through phase binning (top image) and amplitude binning (bottom image), where an example of a 4DCT data set sorted in four breathing phases (0%, 25%, 50% and 75%) is presented. (Adapted from [24])

same anatomic region is scanned repeatedly in order to have information of more than a breathing cycle [26, Ch. 4, p. 65].

As shown in Figure 2.2, without motion information during data acquisition, there is a greater possibility of not knowing where the volume we want to image is and so artefacts will occur. The use of 4DCT images can improve this flaw by using an external respiratory surrogate to monitor and acquire the breathing motion, reducing the chances of having a positional miss.

2.2.4 Treatment planning with 4DCT and International Commission on Radiation Units and Measurements Concepts

For the reason stated above, treatment planning based on 4DCT images is strongly recommended by the European Organisation for Research and Treatment of Cancer [7] for thoracic oncology, since it will be more representative of the tumour position during the time of treatment delivery, allowing for margin reduction and thus less normal lung tissue being irradiated [27]. A typical workflow using 4DCT data for radiotherapy is shown in Figure 2.5.

As it can be seen in Figure 2.5, planning starts by acquiring a 4DCT image of the patient. Through this four-dimensional data sets, it is possible to delineate several volumes related to tumour motion and that are used to plan the treatment. In the International Commission on Radiation Units and Measurements (ICRU) Report 83 it is mentioned that "Delineation of these volumes is an obligatory step in the planning process, as absorbed dose cannot be prescribed, recorded, and reported without specification of target volumes and volumes of normal tissue at risk" [5, p. 41]. Therefore, as reported by Wolthaus *et al.* [27], to determine the target volume, a manual delineation is required in order to get the *Gross Tumour Volume (GTV)*, which is the visible target we want to access, in this case,

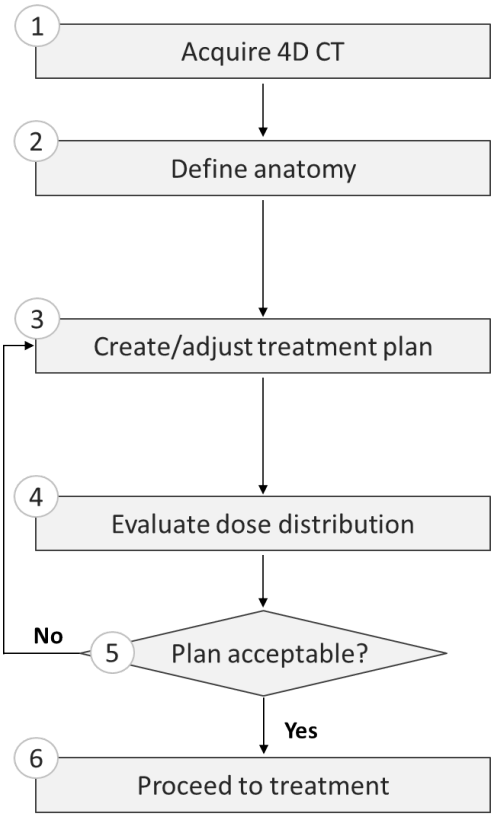

Figure 2.5: Schematic representation of a typical workflow for radiotherapy planning using 4DCT. (Adapted from [22, Ch. 1, p. 13])

the lung tumour. If we account for some "subclinical malignant disease with a certain probability of occurrence considered relevant for therapy" [5, p. 44], then GTV volume plus this margin is called *Clinical Target Volume (CTV)*. Finally, to account for tumour's motion in the organ of study, a new margin is added and the *ITV* concept is defined as "the CTV plus a margin taking into account uncertainties in size, shape, and position of the CTV within the patient" [5, p. 46]. It can also be considered a margin that takes into account both the internal and the setup uncertainties (related with patient positioning and alignment of the therapeutic beams during the treatment planning) [5, p. 46], then we have the *Planning Target Volume (PTV)*, which is used for treatment planning and evaluation (steps 3 to 5 in Figure 2.5). To point out that ITV is considered by the ICRU as an optional tool in helping delineate the PTV. A representation of these concepts is shown in Figure 2.6.

To extract the ITV from a 4DCT data set one can delineate the GTV on each respiratory phase, since CTV is not accessible visually with the current medical imaging methods, and expand it according to the margin needed to get the CTV afterwards. The ITV is then an envelope of the CTV motion [28]. However, this procedure of contouring the GTV increases the workload compared with outlining only one data set. Thereby, post-processing tools, like the Maximum Intensity Projection (MIP), can give a good approximation of the

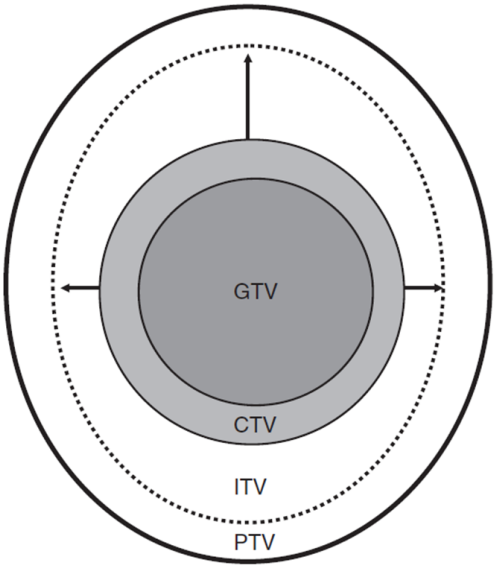

Figure 2.6: Illustration of ICRU volumes' definition: GTV, Gross Tumour Volume; CTV, Clinical Target Volume; ITV, Internal Target Volume; PTV, Planning Target Volume. (Adapted from [26, Ch.2, p. 22])

ITV [28]. What MIP enables is the reduction of all the voxel information, gathered in each respiratory phase from a 4DCT data set, by extracting the CT voxel with the maximum value over each bin [4, Ch. 12, pp. 170-181]. This will generate a single image, with the GTV's motion envelope, which then should have its margins expanded to account for microscopic disease, thus giving rise to the ITV.

After knowing the ITV, it is possible to add the PTV's margin and plan the treatment. It is also possible to calculate the dose from the 4DCT data set by taking average values of the CT voxels [4, Ch. 12, pp. 170-181].

Finally, after preparing the treatment plan and choosing the necessary dose, it is possible to proceed to treatment delivery (step 6 in Figure 2.5), where the patient is placed on the table in the treatment room and where, typically, is aligned to room lasers through skin marks to receive the treatment.

2.2.5 Limitations of 4DCT and Internal Target Volume Uncertainties

Even though the 4DCT is one of the methods that helps achieving specific-time target position, there are some limitations regarding the technique that can lead to ITV's delineation inaccuracies.

Due to collimator limitation and overheating of the X-ray tube in 4DCT acquisition method, a normal scan can be obtained in approximately a minute with a 16-slice CT scanner [2]. This leads to a 4DCT scan that is only representative of the tumour and its motion at that particular time [3] and thus, the treatment plan carries limited motion data. Since normally the patient's breathing pattern is not completely regular, it has

some temporal variations [22, Ch. 1, p. 8], this can lead to the risk of having non-predicted tumour motions during several minutes of treatment delivery. In other words, an incorrect ITV's definition in the CT scan to be used during the treatment later on.

Besides that, artefacts due to irregular breathing are also a topic to consider in 4DCT acquisitions. Since it is known that 4DCT "is affected by variations in respiratory patterns during acquisition" [2, p. 3884], bad delineation of the target volume can also be an outcome from respiration-induced artefacts [29], [30]. In Yamamoto *et al.*'s work [29], these artefacts were already documented and classified into 4 types: blurring, duplicate structure, overlapping structure and incomplete structure, as it can be seen in Figure 2.7.

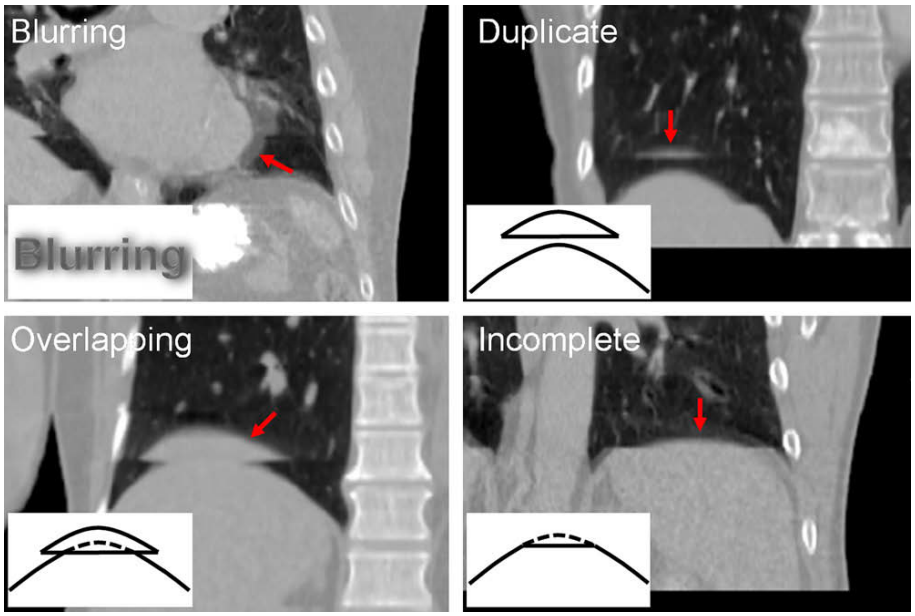

Figure 2.7: Examples of artefacts in 4DCT images due to irregular breathing: blurring, duplicate structure, overlapping structure and incomplete structure. Corresponding artefacts are indicated by red arrows. (Adapted from Yamamoto *et al.* [29])

In addition to what has already been mentioned, it is important to notice that, apart from the irregular breathing that might occur during a treatment session (intra-fractional variation), the patient will also display changes in his breathing pattern between treatment sessions (inter-fractional variation) and, hence, tumour motion, owing to tumour changes in configuration, like its size and position, for example [4, Ch. 12, pp. 170-181]. Also, changes that occur in tumour motion between simulation sessions and treatment sessions can be of importance [2], [31]. All these referred points will result in large uncertainties in the ITV's determination.

Chapter 3

Literature Review

As already stated, the treatment followed by lung cancer patients uses a radiotherapy fractionation of dose procedure, which can be affected by tumour motion, due to patient's breathing. Apart from techniques like PET, which is standardly recommended for use in combination with CT (PET-CT) [3], [20], Dynamic Magnetic Resonance Imaging (dMRI) [20], [32] and Fluoroscopy [2], [3], the use of 4DCT has become a common way to overcome this patient's breathing problem and contour the ITV [2], [3], [22]. The ITV's contouring can be accomplished through the use of MIP method [33], [34], for example, which is then used to create a treatment plan. Therefore, any error in this contouring process can originate a systematic error carried to the patient's treatment. In this sense, the following paragraphs in this chapter will document the studies done so far to point out problems and needs in this area.

3.1 Irregular Breathing in 4DCT

Several studies have already documented how the tumour motion in the lungs occurs [1], [35], [36] and we also know now that 4DCT can account for that motion. However, the current challenge with 4DCT technique is that most lung cancer patients do not breath regularly and so, artefacts will occur in 4DCT acquisition [29], [30]. Since these images are used for treatment planning, it is not convenient that those artefacts persist (see Figure 2.7) as they affect target volumes' representation and delineation.

More recently, studies have been done in order to estimate possible errors in 4DCT caused by irregular breathing, like in Clements *et al.* study [10] which had the aim to image a phantom moving with irregular breathing patterns to determine whether it resulted in errors in volume contouring or alignment in 4DCT and Cone-Beam Computed Tomography (CBCT). The result was banding artefacts in 4DCT MIP images and volume

being underrepresented at the extremes of motion.

In another article, Sarker *et al.* tried to access tumour's position and volume errors in 4DCT through the use of a virtual scanner, designed to reproduce 4DCT images with irregular breathing [9]. They concluded that irregular breathing causes systematic errors in volume and centre of mass measurements during 4DCT simulations. The work also concluded that these errors "are small but depend on the tumour size, motion amplitude, and degree of breathing irregularity" [9, p. 1254], which also confirms Liu *et al.* statement that the tumour motion is highly patient dependent [1].

Besides this intra-fraction variation, articles have also documented the inter-fraction one. Shah *et al.* noted that "daily variations in lung tumour motion between treatment fractions were found to be patient specific" [8, p. 483] proving that discrepancies in tumour position between planning and treatment delivery exist and should be taken into account, by using patient related data. In Liu *et al.* it is mentioned that "patient breathing patterns will likely change during the course of therapy, which will result in large uncertainties in the ITV determination, even if it is done using 4DCT" [1, p. 540]. A statement that was also supported by the result obtained in Britton *et al.*'s work [37], where it was observed an increase in total GTV positional variation over increasing treatment weeks, with similar results for the inter-fractional ITV mobility.

All of these studies documenting irregular breathing patterns were taken into account in the thesis' work by evaluating 4DCT scans in patients with irregular breathing patterns and improving the analysis done so far in the literature by including intra- and inter-fractional information in this study.

3.2 4DCT Accuracy for Internal Target Volume Delineation

Since 4DCT is widely used on radiotherapy to get information about tumour motion associated with respiration, there is a need to know how accurate this technique may be when determining ITV for treatment planning. As stated by Bai *et al.* [38], 4DCT scans should be capable of recording intra-fractional tumour motion and generate accurate ITV.

As many authors depict that patient-specific tumour ITV from 4DCT scans are capable of reducing the risk of missing targets and minimizing unnecessary radiation to healthy tissues, accurate ITV delineation is again enhanced as important. This minimization was found to be true in Rietzil *et al.* article [39], where with the 4DCT technique it was possible to compare its PTV's margins to the ones from helical CT data and note that there was a decrease in target volume sizes, a study case also confirmed by Bai *et al.* work.

Even so, there are works that try to evaluate 4DCT accuracy in determining ITV, since they question whether ITV's definition based on 4DCT simulation is in agreement with the real targets in radiation delivery.

One example is the study done by James *et al.* [40], which tried to demonstrate instabilities in the ITV definition used in clinic based on simulated 4DCT scans acquired in

cine mode. By using patient data, the tumour was modelled as a sphere with 10, 20 and 30 mm of diameter and location extracted from the experimental data. The results from the study demonstrated that ITV values could vary up to 127% for a tumour diameter of 10 mm, 99% for a 20 mm and 69% for a 30mm diameter tumour model.

By comparing the PTVs (which, as it has already been said, are the ITV plus the setup uncertainties margins) acquired from axial 3DCT and 4DCT, Li *et al.*'s work [41] also tried to assess the differences in target position, volume and inclusion relation between a 4DCT-based PTV and 3DCT-based PTV for treatment planning. It concluded that 4DCT-based PTV had a smaller size than 3DCT-based PTV, and the size ratio for the first and second PTV is correlated to the tumour motion vector. These findings can indirectly suggest a similar result for an ITV case, where the ITV from a 4DCT scan would be smaller than the one obtained from a 3DCT scan.

Another similar study, done again by Li *et al.* more recently in 2016, proposed the analysis of the volumetric differences in ITVs obtained with the techniques above mentioned [42]. One aim of the study was to evaluate the accuracy of ITVs defined on 3DCT and 4DCT images of NSCLC patients. Based on an inclusion relation percentage, that uses the ITV from a CBCT scan as a reference volume, both ITVs from 3DCT and 4DCT scans were evaluated. This percentage value showed that for the 4DCT ITV case, 20.04% of the ITV would be irradiated unnecessarily. Whereas, for the 3DCT case, the target size being irradiated unnecessarily was far larger than that when treatment planning was created on 4DCT-based ITV.

Even though the result from this study seems to contradict the former conclusion based on the previous article from Li *et al.*, by showing that 3DCT ITV's definition encompassed a larger ITV than when dealing with the 4DCT one, a crucial point in their analysis was: the fact that the position and shape of targets may be the major factors influencing the inclusion relation. These could be due to respiratory variations in simulation and radiation delivery or even to registration error based on bony anatomy, which may increase the centroid shifts of targets. And so, the article concluded that "The use of the individual ITV derived from 4DCT merely based on bony registration in radiotherapy may result in a target miss" [42, p. 6945].

In Harada *et al.* study [43], the 4DCT technique was used to determine the accuracy of the amplitude of internal fiducial markers in peripheral lung tumours. The article showed that although 4DCT scans can be useful to establish the mean amplitude for a patient during SBRT, they can also underestimate the maximum amplitude during actual SBRT, and so they stated that caution must be paid to determine the internal margin with the 4DCT.

Besides, in another interesting study by Cai *et al.* [44], dMRI was used to assess the accuracy in ITVs determined by 4DCT. By acquiring dynamic images of lung motion based on a magnetic resonance scan, followed by a re-sorting of dMRI images using 4DCT acquisition methods, ITV determination associated with free-breathing cine-mode 4DCT using a simulation method based on dMRI was done. This ITV and the one obtained from

the dMRI data set were compared. The ITVs from the 4DCT simulation method were comparatively smaller than those from dMRI in both phantom studies and lung tumour patient studies, which denotes that the ITV generated from 4DCT tends to underestimate the real value.

The present work aims to provide one more study to assess 4DCT validity in ITVs determination.

3.3 Target Delineation Methods for 4DCT Images

Numerous methods to generate tumour ITV using 4DCT have been documented so far. For example, in Ezhil *et al.* article [28], an optimal approach to delineate patient-specific Internal Gross Target Volume (IGTV) - a concept introduced by the author, "which is the volume containing the GTV throughout its motion during respiration" [26, Ch. 2, p. 23] - from 4DCT images is investigated using 4 different strategies. Whereas, Muirhead *et al.* study [33] led to a better understanding on when to use MIP method in lung cancer patients for ITV delineation.

Normally, GTV delineation in each phase of the 4DCT data set (typically 10 phases) is used to obtain the ITV by combining all 10 individual CTVs, obtained after the expansion of the GTVs, as it has already been described. But, as stated in section 2.2.4, to reduce the workload, there is also the MIP data set approach, which has been widely used in the clinical practice to define the ITV. However, both methods could underestimate or overestimate the true tumour ITV due to the variability in patients' breathing [10], [44]. And besides, it has also been shown by Ge *et al.* that, depending on the delineation method used, the ITV determination can vary significantly [45].

Therefore, the delineation method implemented in the thesis' work was based on a semi-automatic segmentation process developed to extract all of the needed GTVs and summing them to obtain the IGTV. Afterwards, a simple expansion of the IGTV creates the ITV, as mentioned in [26], [28]. This process was thought to be more reliable than the GTVs' delineation based on manual contours, which is subject to an intra- and inter-observer variability in the delineation [46], or the MIP approach, since according to Ge *et al.* "it has been shown that both MIP-based ITV and $ITV_{10Phase}$ could underestimate or overestimate the true tumor ITV because of the variability in patients' breathing" [45, p. 439].

Chapter 4

Methodology

In this chapter, a description of the patients used in the study is given, followed by the image acquisition protocol applied. Then, the proposed algorithm to analyse the images is described as well as the statistical analysis used to validate the results.

Concepts such as *image registration* and *segmentation* are explained here due to its use in the algorithm's development, ITV delineation and extraction are detailed and the used software tool is presented.

4.1 Patients

In the present study, 10 lung cancer patients diagnosed with NSCLC were evaluated at the Uppsala University Hospital, between January and June of 2017.

These patients firstly went through one planning session, where a 4DCT simulation for treatment planning was acquired, followed by three radiotherapy treatment sessions. The treatment was given through the use of SBRT, where a very high irradiation dose is delivered to an extracranial target in one or few treatment fractions [19]. Also, in order not to damage normal critical structures, like the heart or the spinal cord, and target properly the tumour location, CBCT images were used before each fraction of SBRT for corrections in patient's setup. All patients were treated during free breathing without any type of patient guidance and they were classified as patients with an irregular breathing pattern by the medical team.

From the 10 patients included in the study, 5 were selected. If the tumours were diffuse or extensive and if its borders could not be easily detected and differentiated from the adjacent soft tissue, then it was decided that these patients would be excluded from the final analyses. Also, only primary tumour volumes were evaluated. A description of the patients and tumour characteristics is detailed in Table 4.1.

Table 4.1: Characteristics of the patients selected and their respective tumours.

Patient no.	Tumour Location	Tumour Size (cm^3) *	Age	Sex
2	RLL	3.6	73	F
3	RUL	4.3	77	F
6	RUL	1.2	62	M
7	LUL	1.3	76	F
9	RUL	1.2	63	M

Abbreviations: RUL = right upper lobe; RLL = right lower lobe; LUL = left upper lobe; LLL = left lower lobe. * size of the tumour captured during breath-hold.

4.2 Image Acquisition

During the planning session and the first two treatment sessions, extra CT images were acquired, for this study purposes. In each session, a number of 100 axial cine mode 3DCT images, called from now on *cine images*, were obtained as part of the image acquisition method proposed for this study.

To monitor the tumour position during a typical time for treatment delivery, the 100 cine images were acquired during 8 minutes of free breathing. Hence, these cine images would give a more representative look of the tumour positions during an actual treatment session. All these cine images were acquired at a fixed couch position and 50 of those images were selected to be used in the study, since dispersed information from the breathing trace would be provided that way and thus a good coverage of the tumour's random positions.

Apart from acquiring 100 cine images at each of the 3 different sessions, the imaging protocol created for this work consisted of doing, in one of the sessions, a helical 3DCT of the entire thoracic and abdominal region with the patient in breath-hold mode and a helical 4DCT scan also in free breathing, in another session. The CT scanner used for the all protocol was a Philips Brilliance Big Bore (16 Slice).

For the axial cine mode 3DCT, the CT table is kept stationary while several rotations are completed within the duration of the patient's respiratory period (typically 4–6 s), in order to collect images in a similar way to the 4DCT acquisition method. The images were acquired randomly, with no defined time interval between acquisitions, and with a slice thickness of 1.5 mm for all the images.

In the helical 3DCT scans, the CT tube rotates around the patient continuously while the table slides out of the gantry, scanning the patient's body from the lower neck to the upper abdomen, and reconstructing those scans using 0.4 to 1.5 mm slices. The patient is kept under breath-hold during the all process, giving access to both lungs and the whole thoracic anatomy to be imaged. Thus, the produced 3DCT scan could access the tumour volume entirely and therefore was used as the reference image in this study.

For the helical 4DCT imaging technique, it was ensured that an entire respiratory cycle was imaged at each table position, where slices with 1 to 3 mm of thickness were formed. The respiratory trace used for the 4DCT scan reconstruction and binning process was recorded concurrently to scan acquisition by a belt (Philips Pneumatic Bellow) wrapped around the abdomen of the patient. After the image acquisition, the respiratory trace was then used retrospectively to bin and reconstruct the raw 4DCT images, based on a phase binning process, in order to obtain sets of 3DCT images from different breathing phases. In this protocol, 10 respiratory phase 3DCT images were exported for analysis, in an evenly distributed way, over a respiratory cycle. These images were labelled in percent respiratory cycle, 0% corresponding to end-inhalation and 50% corresponding to end-exhalation (see Figure 4.1).

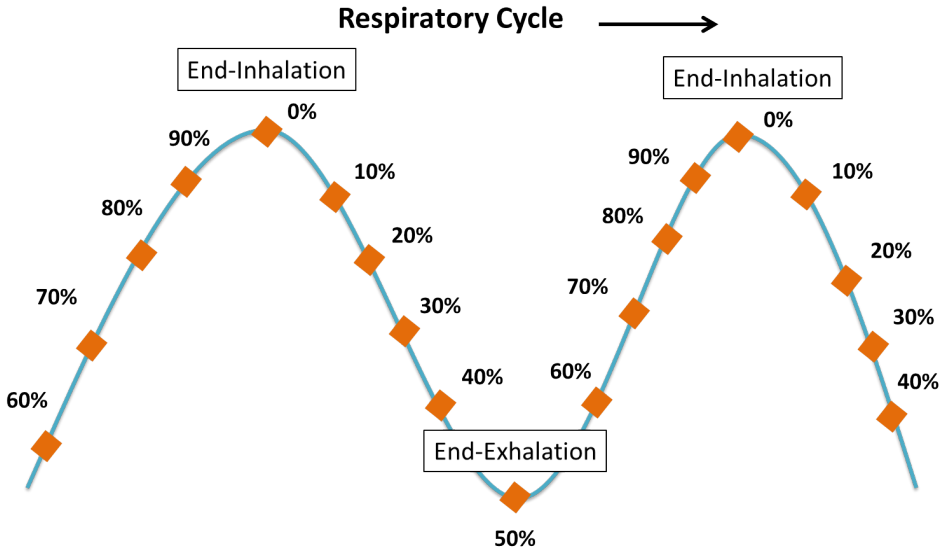

Figure 4.1: Illustration of a breathing trace example labelled according to a 10 phases binning algorithm.

All the acquisitions were performed with the patients in a supine position, with arms extended above the head in supports. The patients' setup was based on skin tattoos and room lasers, mimicking a treatment situation, where the nurses in the CT scanner room aligned the skin marks to the room lasers.

4.3 Image Analysis and Internal Target Volume Estimation

To determine whether patient-specific ITV is accurately represented in the 4DCT images, the data obtained from the 4DCT scan and from the cine images was used to extract and compare the ITV associated to both cases.

The first approach to create an algorithm capable of doing this was executed with resource to MATLAB. However, its development was restrained due to the fact that the time needed to implement all the concepts and functions necessary to obtain the desired ITV would be beyond the stipulated thesis' working plan. Therefore, another toolkit-based software was used, which will be described in section 4.3.5, and a new attempt was done to construct the algorithm needed.

Nevertheless, in order to use and describe how the used software could aid in the algorithm construction, it is necessary to first know what an *image registration* and *segmentation* are and why they were needed.

4.3.1 Image Registration and Segmentation

Since images acquired in different occasions may have a different coordinate system associated to them, meaning that the same anatomical structures may be misaligned once the images are compared, there is a need to find a way to match these images.

This process of finding transformations that relate spatial information conveyed in one image (target image) to those in another (source image) is called *image registration* [47, Ch. 2, p. 12]. By establishing which point in the target image corresponds to a particular point in the source image, the process of image registration is able to align the images and also allows monitoring of subtle changes in size or intensity over time.

There are two main physical categories by which the registration procedure can be classified: *rigid* and *non-rigid* registration. In the first case, for the simplest example of a rigid-body transformation, the images being registered only change position and orientation without changing shape or size, whereas in the second case, the transformation applied enables the deformation of those images, by changing their size and shape [47, Ch. 2, pp. 14-15].

For this study, the simplest rigid transformation was used and so three translations and three rotations would bring the images into registration [48]. It was made sure that this application of a rigid transformation was indeed valid for the study (see Figure 4.2) by checking that the target object in the image that was going to be transformed, from one coordinate system to the other, was not distorted or changed in the spatial relationships between organs in either the source image or the target image [47, Ch. 2, p. 17].

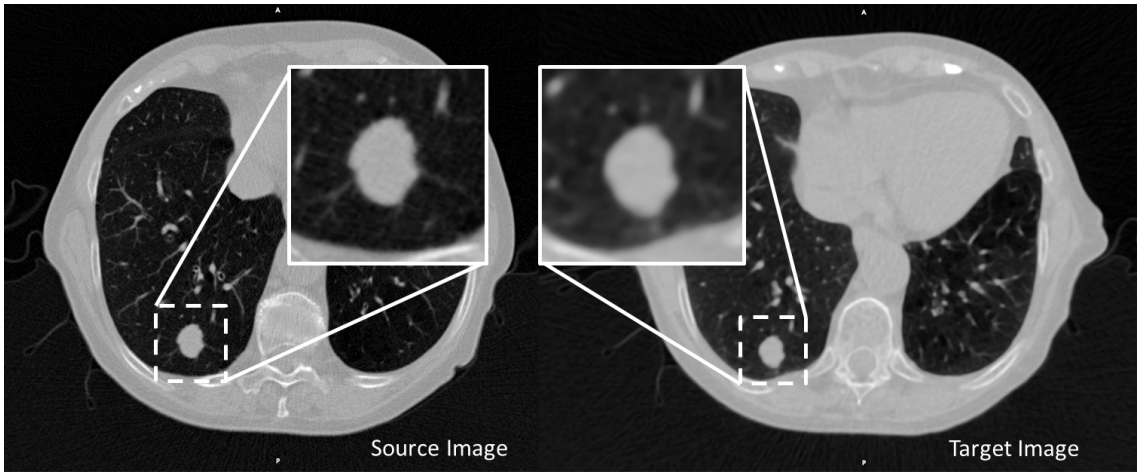

Figure 4.2: The source image, presented in axial view, will be the reference for a rigid transformation of the target image (the images do not have the same resolution). Note that no distortion or change in the spatial relationships between organs has occurred in the target object (see zoomed images) in either of the images, which validates the application of the rigid transformations.

On the other hand, for the ITV to be extracted, the tumour volume and its position in the images have to be accessed. By partitioning an image into regions or objects according to a specified criterion [49, Ch. 3, p. 112], one can find and delineate the tumour volume and position as previously intended. The former definition is known by *image segmentation* and it can be described as a process that includes two tasks: recognition and delineation [50]. Briefly explaining, the first task is related with object spacial localization in the image whereas the second task requires the spatial definition of the object region extent in the image. While humans outperform computer algorithms in most recognition tasks, computers surpass humans in the delineation task [50]. The combination of these human and computer characteristics motivates the use of interactive/semi-automatic segmentation methods that require minimal user assistance for object region detection and computer aid for the delineation procedure [51, p. 9]. In this work, semi-automatic segmentation was employed, where the manual part involved optimization of threshold levels and other segmentation parameters. It was seen in the study, and it had already been documented, that automatic segmentation methods cannot always guarantee complete success. As stated by Falcão *et al.*, "to make them work effectively in a repeated fashion on a large number of data sets often requires considerable research and development" [50, p. 234]. So, a semi-automatic segmentation method was considered a good solution to help in the correct selection and segmentation of the desired target.

4.3.2 Application of Image Registration

In this work, two sets of rigid registrations were used in the algorithm construction: one to align the images to the same coordinate system and another to access the exact tumour position.

In the first set of registrations, since the aim was to get the same coordinate system between the acquired images, bony landmarks in the thoracic vertebrae were selected automatically to be used in the registration process. The assumption was that during an image acquisition these structures would remain static, and so, no distortions would occur associated with the bony landmarks. This way, the bone structures contributed to form a link between acquisitions in the same session, as well as between different sessions.

By doing an image registration based on the same bony landmarks from the cine images, and from the 4DCT data set separately, to the ones found in a reference image, it was possible to align all the images to the same coordinate system, avoiding this way setup errors. The delineation of the respective bony landmarks, from the reference image, the cine images, as well as from the 4DCT data set, was possible thanks to the use of a simple automatic segmentation procedure designed during the study, where a specific threshold level was applied to the images (see Figure 4.3).

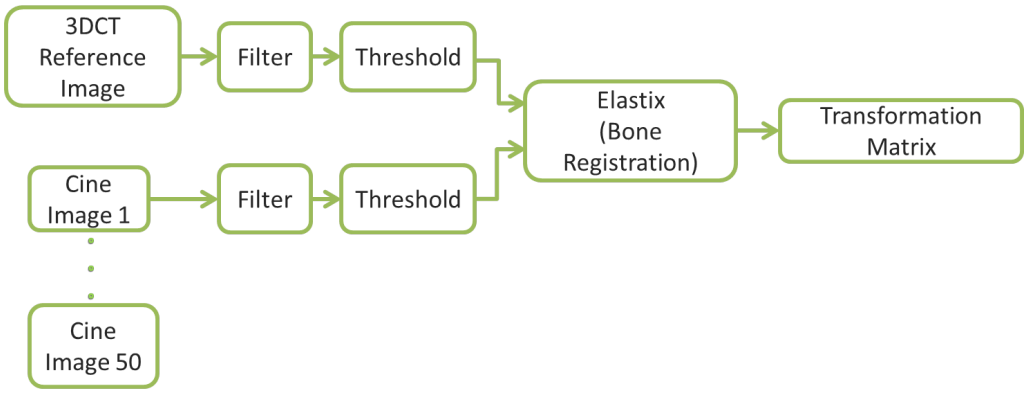

Figure 4.3: Example of a bone registration scheme for the cine images' case of a single session.

From these rigid registration processes, transformation matrices were obtained, as we can see in Figure 4.3. These matrices contain information about the transformations that should be applied to the cine images, or the 4DCT data set, in order to align them to the same reference. The process described so far will be referred to as *bone registration* from now onwards. The result from the bone registration steps, presented in Figure 4.3, can be seen in Figure 4.4.

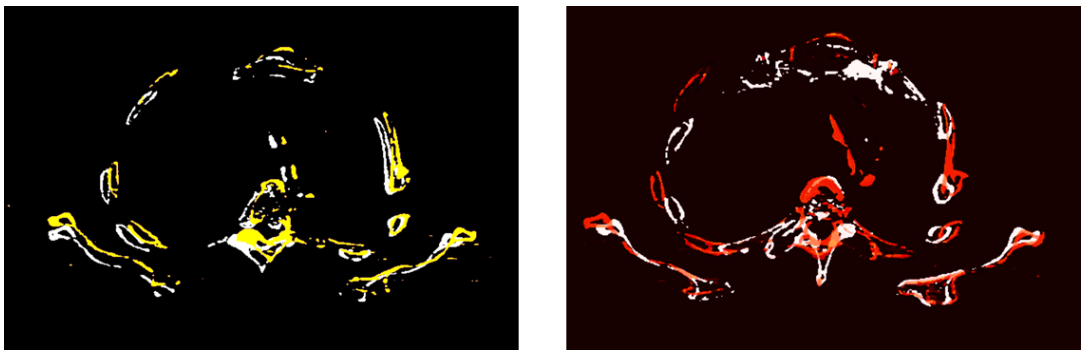

Figure 4.4: Example of a bone registration from Patient 3. The cine image (colorful bony structures in both images) without alignment is presented in the left image and, after it was matched to the reference image (white bony structures in both images), the result is present in the right image. There, one can see the correct alignment between the images in the axial perspective.

After making initial transformations in the cine images and 4DCT to align the bones to the same reference image, it is then possible to extract the tumour position when the image was acquired under the same coordinate system. Even so, a second registration was necessary in order to know the exact tumour position, as it will be explained in the next section.

These two mentioned sets of registrations, together with known methods for image analysis, such as filtering and thresholding methods, would lead to tumour's extraction and ITV delineation after implementing them in the algorithm.

The algorithm was mainly conceived to semi-automatically segment the tumour from the 3DCT 10 phases' images of the 4DCT data set and from the 50 cine images data set from each of the three sessions. In addition, aside from the bone registration step described, the steps implemented in the algorithm were thought to give a process as similar as possible between the cine images and the 4DCT case. Some adjustments had to be done in these steps, however, based on the limitations each set of images had, as we will depict later on. The following sections will describe the steps applied to construct the semi-automatic segmentation algorithm for each data sets of images.

4.3.3 Internal Target Volume Segmentation - 3DCT Data Set

For the cine images case, since the CT scanner could only provide three-dimensional images that cover 24 mm of the thorax in the craniocaudal direction, a clinical limitation, a very restricted view of the tumour volume was obtained.

To overcome the narrowness described, the reference image was also used here as a model, to give access to the entire tumour volume and tumour motion extension (the reference image chosen for this study was the 3DCT image taken during breath-hold, as mention briefly in section 4.2).

The implementation of the ITV's segmentation procedure for the cine images case is schematically shown in Figure 4.5, where the following steps were used:

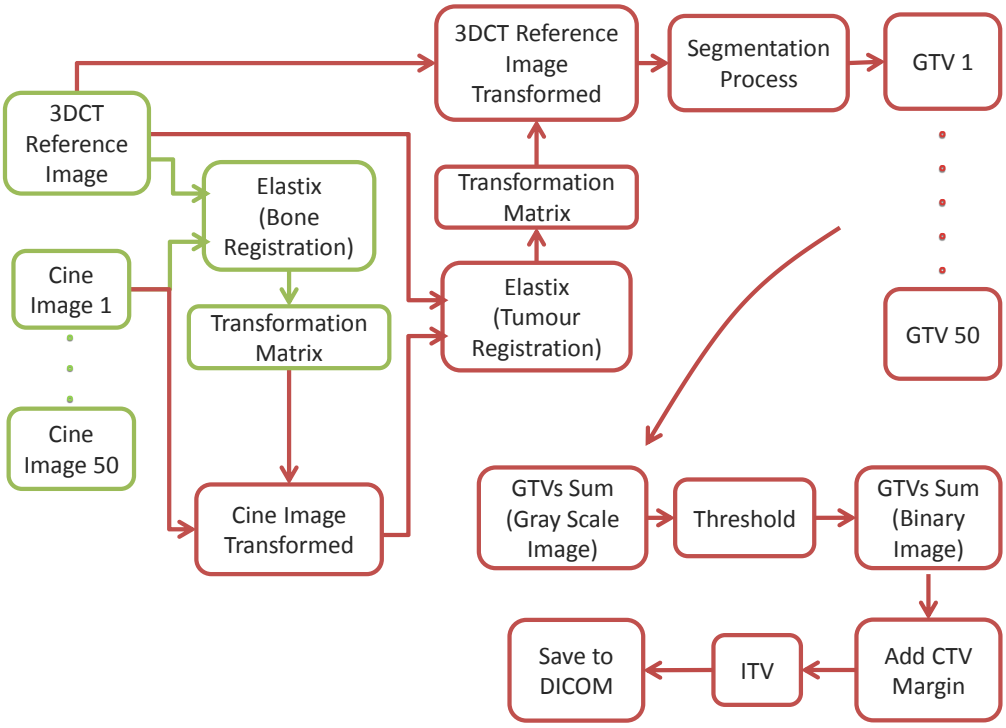

Figure 4.5: Schematic representation of the ITV segmentation procedure from a cine images single session case.

1. The bone registration, described before in section 4.3.2, was applied between the 50 cine images from each session and the reference image, in order to get the transformation matrices that would enable the alignment of the cine images according to the reference image coordinate system.

2. In order to find the extent of the tumour displacement in each cine image, the tumour present in the reference image was registered to the corresponding part in the cine image, in a process that will be referred to as *tumour registration*.

   Note: It was also assumed here that the small volume of the tumours analysed would not need to be distorted or changed in order to the corresponding tumour present in the reference image to match it, and so, a rigid transformation was also applied in this case.

3. The 50 rigid transformation matrices that resulted from the last registration process were then applied on the reference image to create a set of 50 transformed reference images.

4. To each of the transformed reference images is then applied a segmentation process, where thresholds, dilation masks and erosion masks are used, in order to extract the tumour volume, which in this case represents the GTV. The output from this step is a binary image from each of the 50 GTVs.

5. By summing this set of 50 GTVs from different transformed reference binary images, a single gray scale image with the volume occupied by the tumour motion extension was obtained (which corresponds to the IGTV). This final image was then converted to a binary image, by setting a threshold level of 95% of the maximum voxel intensity.

6. The addition of a 0.8 cm uniform margin in the binary image obtained previously (to take into account the CTV), gave us the resulting ITV's image from a cine images single session (see Figure 4.6), after saving it in a Digital Imaging and Communications in Medicine (DICOM) file format.

The size of the CTV's margin employed in this work was determined based in the literature [26], [28], [52], even though it is known that controversy regarding inconsistency in CTV definition exists [19], [53] and that this margin is not used in some centers [53].

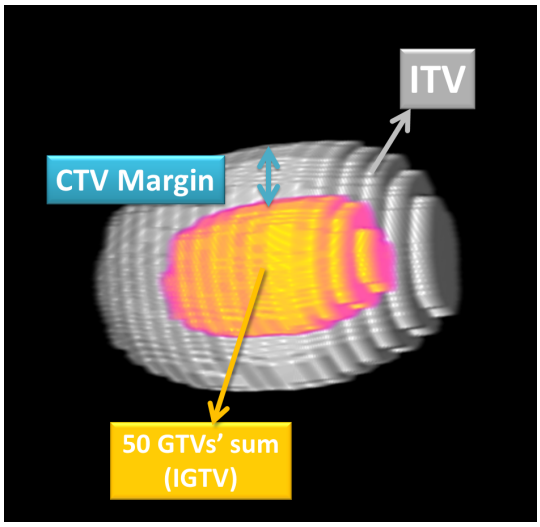

Figure 4.6: Three-dimensional representation of the resulting ITV after adding the 0.8 cm CTV's margin to the 50 GTVs' sum (IGTV) binary image from Patient 2.

4.3.4 Internal Target Volume Segmentation - 4DCT Data Set

To obtain the ITV from the 4DCT images, two methods were implemented. The purpose was to retrospectively compare the 4DCT ITV achieved from two different strategies. In general, Method 1 segments the tumour directly from each phase and Method 2 transforms the segmented tumour from the breath-hold reference CT according to the tumour position in each phase.

Method 1 - Individual tumour extraction: In all of the 10 phases 3DCT scans from the 4DCT data set, the tumour is extracted individually, after the visual verification that the bone registration between the 4DCT and the reference image was correctly accomplished. In this bone registration step, an average representation of the bony landmarks from

all the phases of the 4DCT data set was used in order to improve the outcome from the registration process. By applying a new, and specific, segmentation procedure to extract the tumour to each of these 10 3DCT scans, it was ensured that each binary image obtained contained the tumour correctly contoured. Besides, this individual tumour extraction was also checked visually. The segmentation procedure, like in the cine images case, used thresholds, dilation and erosion masks in order to extract the GTV. Afterwards, all of the 10 GTVs extracted were summed and, by setting a threshold level of 95% of the maximum voxel intensity, a single binary image was obtained (with the IGTV representation). An extra 0.8 cm margin was also added here in order to account for the CTV, giving as a result an image containing the ITV (see a schematic representation of the method in Figure 4.7).

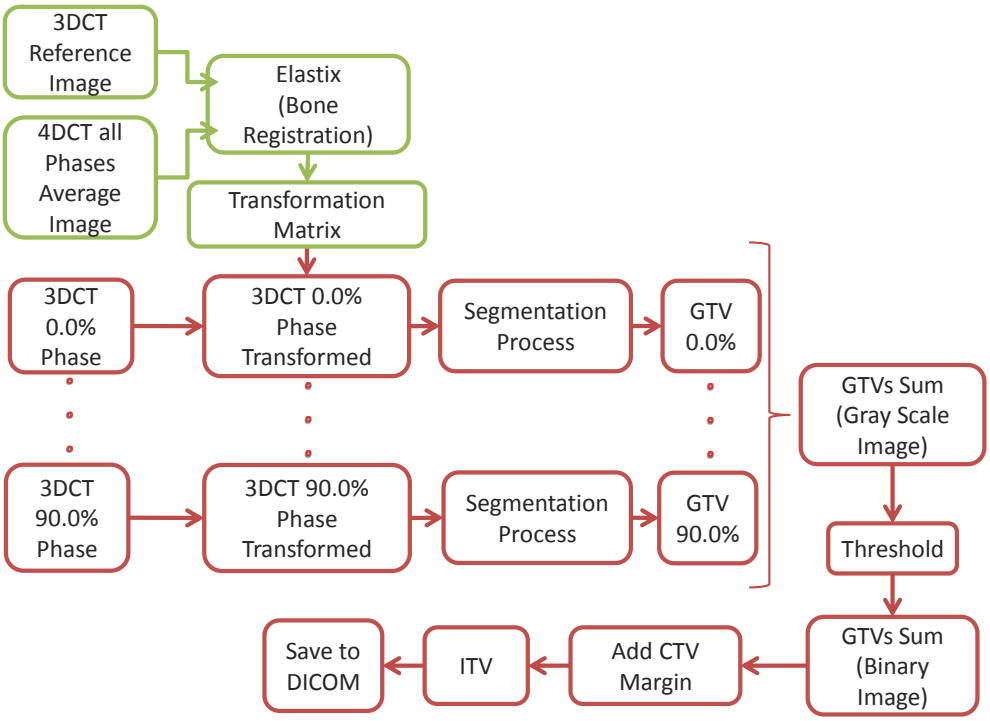

Figure 4.7: Schematic representation of the ITV segmentation procedure from the 4DCT Method 1 case.

Method 2 - Cine images based extraction: Following a similar procedure as the one from the cine images, firstly, the average representation of the bony landmarks of the 4DCT data set undergoes bone registration, according to the reference image. Secondly, the information obtained from that registration process is applied to each of the 10 phases 3DCT scans from the 4DCT data set, resulting in 10 3DCT transformed images. Hereafter, each of the transformed images goes through tumour registration, where the reference image is the one being registered to each of the transformed images. This procedure allows the extraction of the same tumour volume as the one obtained from the cine

images, only displaced in different directions. In this method, the selection of the set of transformations used to extract the tumour (thresholds, dilation masks, erosions masks, etc.) was the same as the one in the cine images case, in order to make the process as similar as possible. In the end, as before, all the 10 tumour volumes extracted were summed (creating the IGTV), a threshold level of 95% applied, and an extra 0.8 cm margin added, in order to obtain one binary image that had the ITV (see a schematic representation of the method in Figure 4.8).

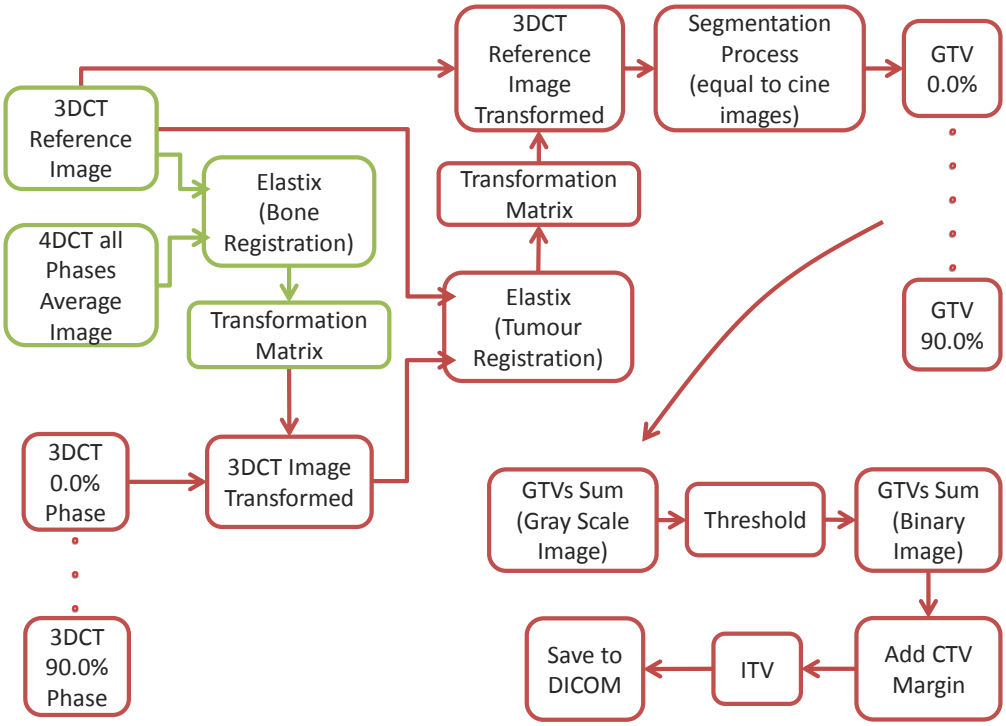

Figure 4.8: Schematic representation of the ITV segmentation procedure from the 4DCT Method 2 case.

In the end of each method, the single binary image was saved in a DICOM file format.

4.3.5 Image Analysis Software

The image registration process and ITV segmentation so far described were constructed, and implemented, with recourse to the Medical Interactive Creative Environment (MICE) application. MICE is a powerful toolkit for image data analysis, developed in Umeå University Hospital, Sweden. It allows the creation of our own calculation process in a node-based graphical interface; importation of different types of files and folders in DCM, JPG, BMP, etc.; registration support via Elastix; use of Insight Segmentation and Registration Toolkit (ITK) filters; implementation of basic arithmetic of three-dimensional volumes; mask generation for faster calculations; use of basic statistics; exportation of data to DICOM, MHD, JPEG, Excel; as well as many other functionalities [54].

Even though diverse toolkits exist nowadays to assist researchers in there medical image registration work, like ITK, Elastix, Advanced Normalization Tools, NiftyReg, etc. [55], the main reason for the use of MICE in this study was due to the fact that this program joins many of the popular toolkits together in a clear and efficient node-based work flow chart. For example, it enables the application of different types of transformations to the medical images used, such as the registration process, via Elastix program. In addition, its interface is configured in a very user-friendly way. An illustration of MICE interface is presented in Figure 4.9, at the end of the chapter.

4.3.6 Extracting the Internal Target Volume

The final result from the ITV segmentation in Method 1 ($ITV_{Method\ 1}$), Method 2 ($ITV_{Method\ 2}$) and in the cine images ($ITV_{Cine\ Images}$) was, as described in the sections 4.3.3 and 4.3.4, a single binary image with the total volume occupied by the tumour motion from a patient in a free breathing condition. In order to access the values of the resultant volumes in cm^3 a MATLAB script (version R2012b, The MathWorks Inc) was written. This script takes into account the amount of white pixels in all the slices of the binary image and converts the total value to a volume, based on the image resolution information included in the DICOM file.

4.4 Statistical Analysis

From the procedure described in the sections above, the ITV's value from the cine images and from the two segmentation methods used in the 4DCT data set was obtained. After extracting the ITV values in each method, simple volume assessment can be accomplished. Firstly, absolute volume measurements were observed. Hereafter, in order to evaluate and compare these ITVs' values statistically, a Wilcoxon Signed-Rank Test was used.

4.4.1 Statistical Test Selection

In this study, there was the aim of checking if the ITV acquired from the 4DCT data set could underdose the tumour in radiotherapy treatments.

Having collected clinical data to verify this, there should be a procedure by which it would be objectively confirmed if this statement is true or not. Therefore, based on Siegel steps, that will be presented below (for further details see [56, Ch. 2, 3 and 5]), the reason for the statistical test used will be clarified:

1. **State the null hypothesis.**

   The null hypothesis (H_0) is used in statistics to state that a given claim about a population parameter is true. It is normally formulated with the intention of being rejected. If it is proved that H_0 is false, then an alternative hypothesis (H_1), that

usually opposes H_0, will be accepted as true. In the present context these are the hypotheses formulated:

$\Rightarrow H_0$: 4DCT data set's ITV is bigger or equal to the cine images' ITV.

$\Rightarrow H_1$: 4DCT data set's ITV is smaller than cine images' ITV.

In other words,

H_0: $\text{ITV}_{\text{4DCT Images}} \geqslant \text{ITV}_{\text{Cine Images}}$ ***vs*** H_1: $\text{ITV}_{\text{4DCT Images}} < \text{ITV}_{\text{Cine Images}}$

2. **Choose a statistical test (with its associated statistical model) for testing H_0.**

   In order to choose a statistical test, it is important to notice that no previous information about the distribution or parameters of the population being analysed are known. In this context, a nonparametric statistical test is ideal since it "is a test whose model does not specify conditions about the parameters of the population from which the sample was drawn" [56, Ch. 3, p. 31].

   Because the aim is to compare the ITVs obtained through two different methods (4DCT data set and cine images), but from the same patient, the resulting two ITV values - one from each method (sample) - are collected from the same source (patient) and, thus, are dependent. That is why these samples are called dependent, paired or matched samples [57, Ch. 10, p. 440].

   From the existing nonparametric tests for two related samples, the Wilcoxon Signed-Rank Test was chosen because it can be used when the differences between sample pairs do not follow the assumption of normality, but "it can be assumed that the differences are a random sample from a continuous symmetric distribution" [58, Ch. 11, p. 466], allowing the test of hypotheses about the median difference (M_d = Median($\text{ITV}_{\text{4DCT Images}}$ - $\text{ITV}_{\text{Cine Images}}$)). The hypotheses test is now presented as:

   $$H_0: M_d \geqslant 0 \ \textbf{\textit{vs}} \ H_1: M_d < 0$$

3. **Specify a significance level (α) and a sample size (N).**

   A significance level is a small probability that specifies the region of rejection of a test. It is symbolized by α and if the value obtained from the statistical test applied has a probability of occurrence under H_0 equal to or less than α, we chose to reject H_0 in favour of H_1 [56, Ch. 2, p. 8].

   In the present case, since a Wilcoxon Signed-Rank Test was chosen, the sample size is going to influence the choice of α. For a sample size of N = 5 (Wilcoxon test is for a small-sample case) the value for the significance level will be $\alpha = 0.05$ for a one-tailed test and $\alpha = 0.10$ for a two-tailed test [59, Ch. 19, p. 975].

4. **Find (or assume) the sampling distribution of the statistical test under H_0.**

   Since the number of samples is small, the only assumption done about the distribution is that it is symmetric.

5. **On the basis of (2), (3) and (4) above, define the region of rejection.**

   The region of rejection "consists of a set of possible values which are so extreme that when H_0 is true the probability is very small (i.e., the probability is α) that the sample we actually observe will yield a value which is among them" [56, Ch. 2, p. 13]. If H_1 indicates the predicted direction of the difference then a one-tailed test is used, otherwise it is applied a two-tailed test. For this study purposes, a one-tailed test is used since $H_1 : M_d < 0$ and so a value of $\alpha = 0.05$ is chosen to define the region of rejection.

6. **Compute the value of the statistical test using the data obtained from the sample(s). If the value is in the region of rejection, the decision is to reject H_0; if the value is outside the region of rejection, the decision is to accept H_0.**

4.4.2 Wilcoxon Signed-Rank Test

Briefly explaining the test chosen, after having selected the hypotheses to test (adapted from [59, Ch. 19, p. 974]):

1. Calculate the difference, D_i, between the N matched pairs values .
2. Rank the absolute values of the N differences from the smallest (rank 1) to the highest (rank N).
3. Omit the differences equal to zero and reduce the number N accordingly.
4. Calculate the rank sum T^- of the negative differences and the rank sum T^+ of the positive differences.
5. For a one-tail test in the lower tail ($H_1 : M_d < 0$), reject the null hypothesis if the computed T^+ test statistic is less than or equal to the critical value T_0 (region of rejection):

   $$T^+ \leqslant T_0 \ ,$$

   where T_0 is a value already calculated and tabulated. To choose the critical value one must know the sample size, the type of tail (one or two-tailed) and the significance level of the test.

Note: If two or more differences are equal, assign each of them the mean of the ranks they would have been assigned individually if no ties had occurred.

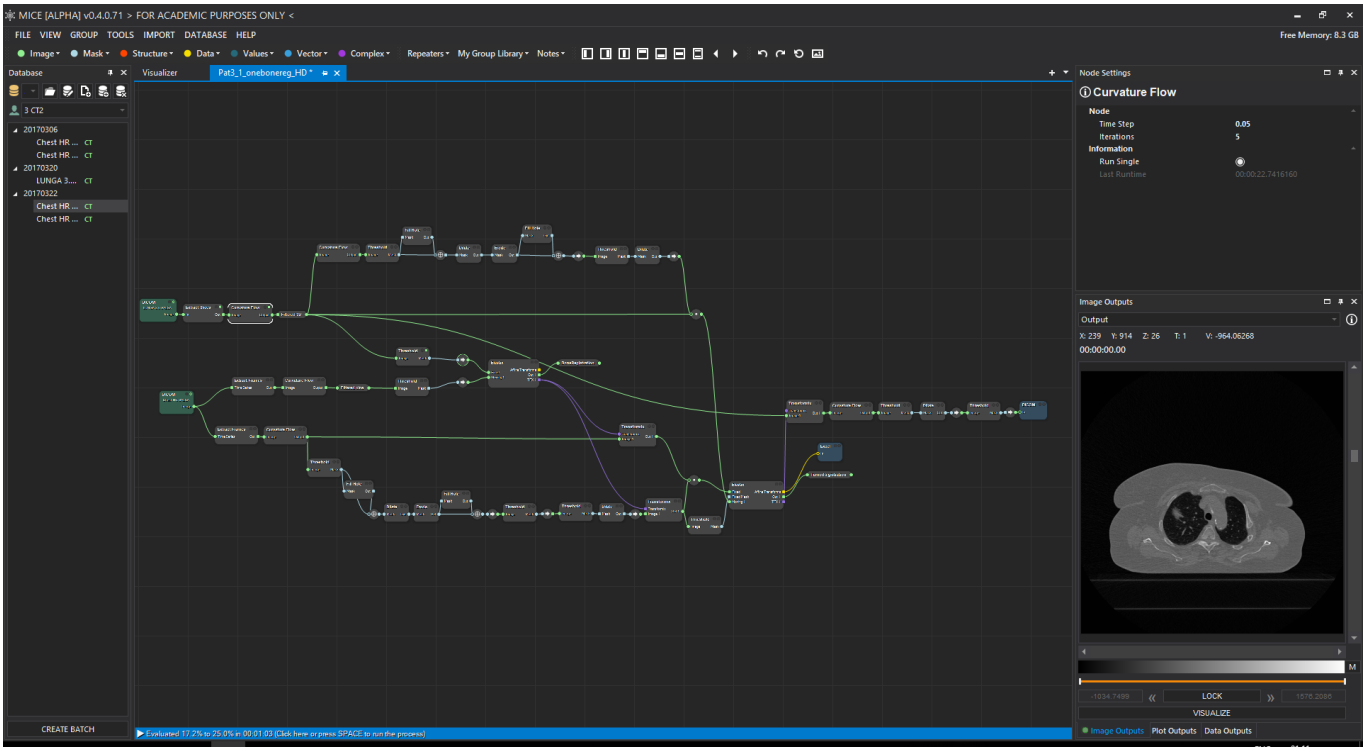

(a) Node-based graphical interface

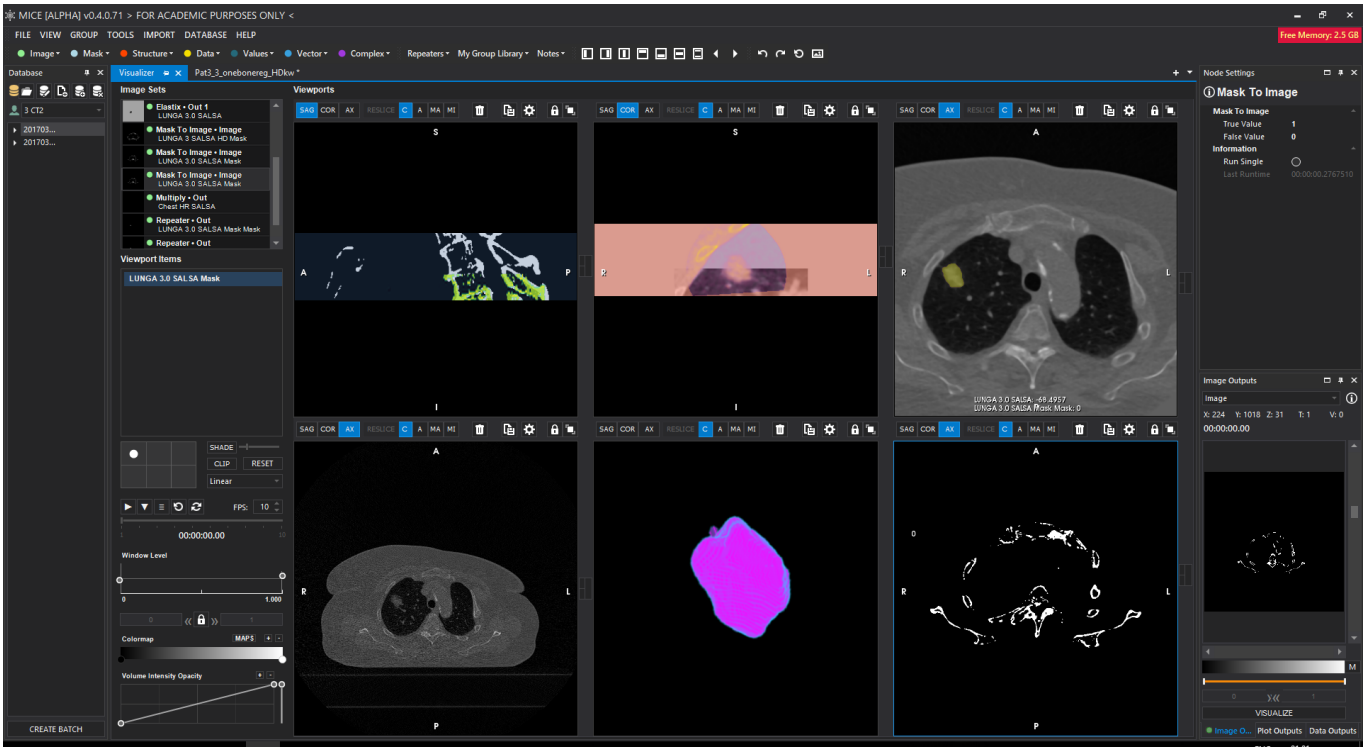

(b) Visualizer interface

Figure 4.9: MICE software with the corresponding two views of the interface.

CHAPTER 5

Results and Discussion

5.1 Internal Target Volume Results Analysis

The implementation of the ITV segmentations described in the previous chapter led to the results presented in Table 5.1. The sum of the ITVs from the 3 sessions equals the $ITV_{\text{Cine Images}}$. In this faction, both intra- and inter-fractional motions affect the $ITV_{\text{Cine Images}}$, hence it represents a good estimate of the clinical treatment scenario.

Table 5.1: ITV results from the cine images, Method 1 and Method 2 cases.

Patient no.	$ITV_{\text{Cine Images}}$ (cm^3)	$ITV_{\text{Method 1}}$ (cm^3)	$ITV_{\text{Method 2}}$ (cm^3)
2	47.6	47.4	41.9
3	45.6	40.2	36.7
6	24.4	20.9	20.4
7	27.0	24.7	18.6
9	24.4	23.4	19.9

It can be pointed out, from Table 5.1, that the volumes obtained in the 4DCT segmentation (Method 1 and 2) appear to be smaller than the ones obtained in the cine images case. By applying the Wilcoxon Signed Rank test to check the former observation, Table 5.2 was constructed.

Table 5.2: Wilcoxon Signed Rank Test between Method 1 ITV and and cine images ITV, as well as between Method 2 ITV and cine images ITV.

Patient no.	**2**	**3**	**6**	**7**	**9**
ITV$_{\text{Method 1}}$	47.4	40.2	20.9	24.7	23.4
ITV$_{\text{Cine Images}}$	47.6	45.6	24.4	27.0	24.4
Difference (D_i)	-0.2	-5.4	-3.5	-2.3	-1.0
$\lvert D_i \rvert$	0.2	5.4	3.5	2.3	1.0
Rank	1	5	4	3	2
Rank Sum		$T^+ = 0$	$T^- = 15$		
ITV$_{\text{Method 2}}$	41.9	36.7	20.4	18.6	19.9
ITV$_{\text{Cine Images}}$	47.6	45.6	24.4	27.0	24.4
Difference (D_i)	-5.6	-8.8	-4.0	-8.5	-4.5
$\lvert D_i \rvert$	5.6	8.8	4.0	8.5	4.5
Rank	3	5	1	4	2
Rank Sum		$T^+ = 0$	$T^- = 15$		

Since N = 5 and for $\alpha = 0.05$, we get $T_0 = 1$ (retrieved from table of critical values in [59, Ch. 19, p. 975]). Therefore, the null-hypothesis can be rejected in both cases, since for both tests $T^+ = 0$, and so, $T^+ \leqslant T_0$ (region of rejection).

This means that the median of the 4DCT ITV, in either of the methods, is statistically significantly smaller (at a 5% level) than the median of the cine image distribution, i.e., the ITVs from the 4DCT methods are indeed smaller than the ones obtained by the cine images method.

A brief look in Table 5.1 also shows that Method 1 gives bigger ITVs than Method 2 and hence closer results to the ITV obtained from the cine images case. Therefore, Method 1 was used to represent the 4DCT case and do another assessment: to compare the ITV$_{\text{Method 1}}$ with the ITV$_{\text{Cine Images}}$ from each session individually.

The previous ITVs from the cine images case, presented in Table 5.1, were obtained from the sum of ITVs from 3 different sessions and so that value might be different from the one obtained from each individual session. The purpose of this new comparison was to verify if the 4DCT acquisition's ITV would still give an underestimated value once compared with the ITV produced from the cine images from different days. The values of the ITVs obtained from each individual session are shown in Table 5.3.

Table 5.3: ITV results from Method 1 and cine images' different sessions.

Patient no.	$\mathbf{ITV_{Method\ 1}}$ **(cm^3)**	$\mathbf{ITV_{Session\ 1}}$ **(cm^3)**	$\mathbf{ITV_{Session\ 2}}$ **(cm^3)**	$\mathbf{ITV_{Session\ 3}}$ **(cm^3)**
2	47.4	41.3	42.7 *	43.6
3	40.2	40.4 *	39.8	42.2
6	20.9	24.2 *	23.5	18.6
7	24.7	24.2 *	24.7	27.5
9	23.4	23.3 *	25.1	24.7

* ITV values from the same day as the 4DCT acquisition.

Apart from patient 2, where the 4DCT scan was taken in the same day as the second session, the other patients had the 4DCT scan taken in the first session.

After analysing Table 5.3, it can be noticed that only in the case of patient 3 and 6 the ITV value from the 4DCT acquisition was smaller than the cine images acquisition for the same day. In the remaining cases, the 4DCT ITV did not seem to be underestimated when compared with the cine images' ITV of the same day. Therefore, it does not seem to exist a common behaviour on the observed data sets for the same session.

In addition, once the Wilcoxon Signed Rank test was again implemented to verify the null hypothesis between the $ITV_{Method\ 1}$ with the $ITV_{Cine\ Images}$ from each individual session (see Table 5.4 in the next page), the 4DCT method exhibited no signs of underestimating the ITV compared to the ITVs from the cine images in the three sessions. This time, for the same region of rejection and critical value, we accept the null hypothesis in all of the cases and conclude that through the statistical evaluation done, the 4DCT method does not underestimate the ITV when the volumes comparison is between the 4DCT method and each cine images' individual session. So, it seems reasonable to say that the test suggests that, in general, 4DCT scans can take into account intra-fractional movements of the tumour.

The situation presented here seems to show that a single 4DCT, taken before treatment, may not account for inter-fractional changes over a treatment time (it was shown an underestimation of the 4DCT ITV from the first Wilcoxon test), but it seems to generally be able to encompass the variable changes within individual sessions (statistical conclusion from the second Wilcoxon test). Therefore, regarding the first question presented in this thesis, it seems reasonable to say that the ITV obtained from a 4DCT scan can indeed differ from the one we get from the image acquisition method proposed for this study (cine images case). However, the difference in the conclusions taken above, leads us to think about its possible causes and hence, the second topic approached by this thesis: *Can we identify the factors that influence the ITV construction?*

Table 5.4: Wilcoxon Signed Rank Test between Method 1 ITV and the ITVs obtained in different sessions.

Patient no.	**2**	**3**	**6**	**7**	**9**
ITV$_{\text{Method 1}}$	47.4	40.2	20.9	24.7	23.4
ITV$_{\text{Session 1}}$	41.3	40.4	24.2	24.2	23.3
Difference (D_i)	6.1	-0.2	-3.3	0.6	0.1
$\lvert D_i \rvert$	6.1	0.2	3.3	0.6	0.1
Rank	5	2	4	3	1
Rank Sum		$T^+ = 9$	$T^- = 6$		
ITV$_{\text{Method 1}}$	47.4	40.2	20.9	24.7	23.4
ITV$_{\text{Session 2}}$	42.7	39.8	23.5	24.7	25.1
Difference (D_i)	4.7	0.4	-2.6	0.0	-1.7
$\lvert D_i \rvert$	4.7	0.4	2.6	–	1.7
Rank	4	1	3	–	2
Rank Sum		$T^+ = 5$	$T^- = 5$		
ITV$_{\text{Method 1}}$	47.4	40.2	20.9	24.7	23.4
ITV$_{\text{Session 3}}$	43.6	42.2	18.6	27.5	24.7
Difference (D_i)	3.7	-2.0	2.2	-2.8	-1.3
$\lvert D_i \rvert$	3.7	2.0	2.2	2.8	1.3
Rank	5	2	3	4	1
Rank Sum		$T^+ = 8$	$T^- = 7$		

5.2 Influences in the Internal Target Volume Construction

In order to get a valid comparison between the ITVs from the 4DCT scans and from the cine image data set, it was ensured that the algorithm implemented to extract the tumour volume, and create the corresponding ITV, was based on the same principles and would lead to a final process as similar as possible between both cases.

Even so, it was observed that the construction of the ITVs in either set of images can be influenced by the type of information (same day or different days) and quantity (number of images) gathered to form the ITV.

Since the 4DCT ITV was obtained based on information from a single session, it only contains intra-fractional variations information. So, in order to explore and study the influence of different days gathered information in the ITV construction (inter-fractional variation), the cine images case was used. The goal was to compare the result obtained from different days gathered information ITV with the 4DCT ITV. This analysis, and the ones that follow, were based on Patient's 7 case since he seemed to provide this discussion with a good example.

In Figure 5.1 the inter-fractional analysis done to Patient 7 is presented and it can be noticed that from the ITV produced in the first session, to the ITV obtained from the summed information of the first and second session, the final ITV did not changed

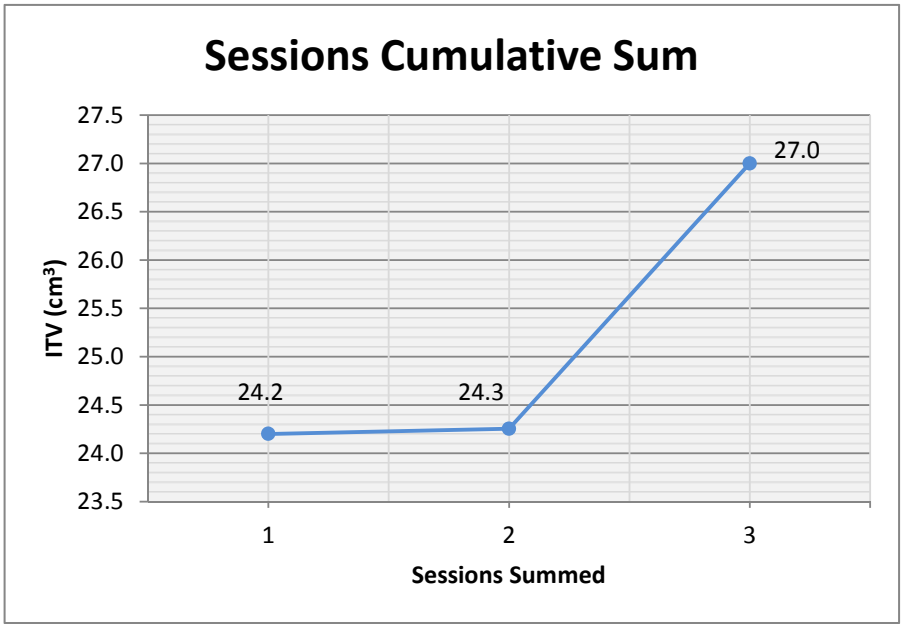

Figure 5.1: Inter-fractional changes in ITV value from Patient 7 using the $ITV_{Cine\ Images}$, from different sessions, summed cumulatively: firstly the session 1 ITV is presented, 24.2 cm^3; then the joint ITV result from sessions 1+2, 24.3 cm^3; finally the session 3 is added to create an ITV with 1+2+3 sessions information, 27.0 cm^3.

significantly. However, by joining the third session, a 11% increment was added to the ITV's final result.

Visual inspection of the breathing traces from each session allowed to conclude that a change occurred in the third session breathing amplitude (it increased from 5 to 10mm, approximately), which influenced the ITV's final value (see Figure 5.2).

In a clinical context it can then be foreseen that during the course of a treatment, which can take several days or weeks, the 4DCT ITV created based in a certain session might mislead about the ITV value achieved in a different session [31], [37]. A reason for this might be that the same patient can breathe differently according to his physical condition that day, which leads to a different type of breathing pattern from session to session (inter-fractional variations), and with an even more noticeable breathing pattern in the case of patients in which the breathing trace is not regular at all.

However, it should be noticed that this conclusion only holds if no baseline shift influenced the three days based cine images' ITV. So, it is important to check for any changes in the alignments between the three volumes that form the $ITV_{Cine\ Images}$.

In the present case, a baseline shift correction led to a decrease in the cine image's ITV value, from 27.0 cm^3 to 25.4 cm^3 (see Figure 5.3). Nevertheless, this reduction did not change the general conclusion taken in section 5.1 that the 4DCT ITV, in both methods used, continues to be smaller than the ITV from the cine images case (24.7 cm^3 < 25.4 cm^3, for method 1, and 18.6 cm^3 < 25.4 cm^3, for method 2), even after the baseline shift correction.

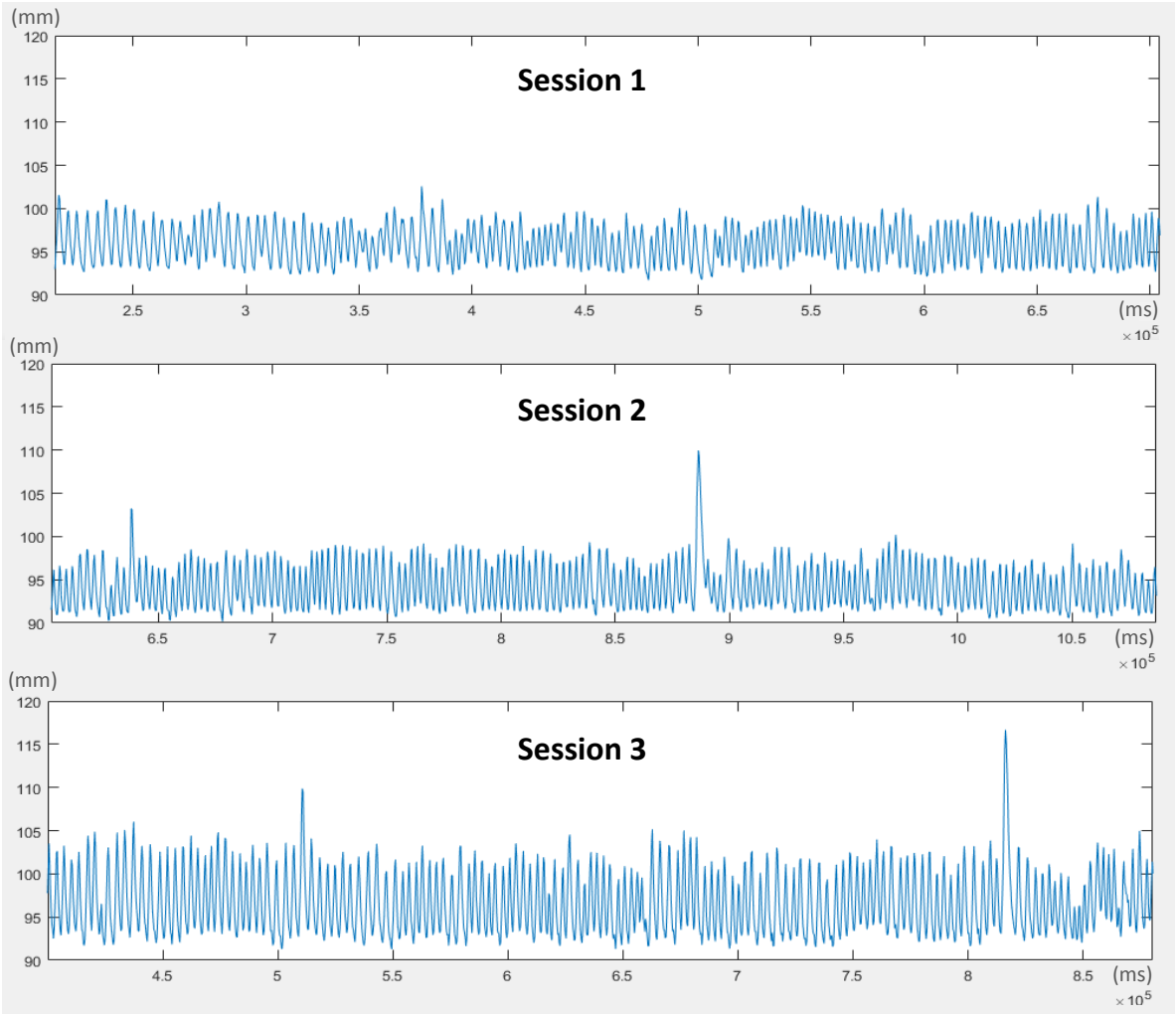

Figure 5.2: Intra- and Inter-fractional changes in the breathing pattern of Patient 7 across 3 different sessions. The breathing information was acquired concurrently with the image acquisition in each session.

These baseline shifts might result, for example, from changes between abdominal and chest breathing, which were observed during acquisition time and between sessions, or from the relaxation of the patient during the procedure, a situation also described in some articles [6], [60]. The shifts can also exist due to poor bone registrations, which would affect the resulting tumour's location. However, this was not considered as a cause since the bone registration was always evaluated and corrected visually.

Another topic to consider in this influence to the ITV's final value, besides the day-to-day breathing pattern changes (inter-fractional variations), is the breathing pattern changes within a session (intra-fractional variations).

During the visual inspection of the ITV created in a single acquisition session, also from the cine images case, it was seen that, even during the same session, the breathing

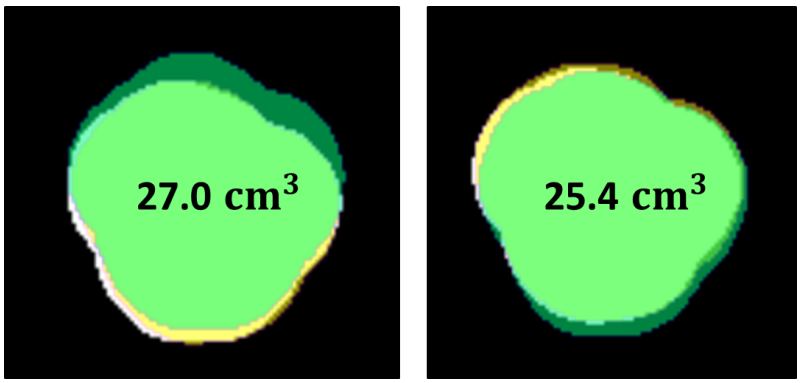

Figure 5.3: Example of axial view summed ITVs in the cine images' case from Patient 7, with baseline shift (left) and without baseline shift (right) between 3 different sessions: session 1 (white area), session 2 (yellow area) and session 3 (green area). The correspondent ITV's value is also shown in each image.

cycle variability can progressively lead to different ITV values.

By observing the cumulative sum of 50 cine images from the third session of patient 7, which was the most variable one, this phenomenon can be illustrated (see Figure 5.4). This cumulative sum was done sequentially, by summing equally spaced sets of 10 images from the beginning of the acquisition until the end, up to a total of 50 images. The use of 50 images instead of 100, allowed the use of more dispersed information from the breathing trace and thus a good coverage of the tumour's random positions.

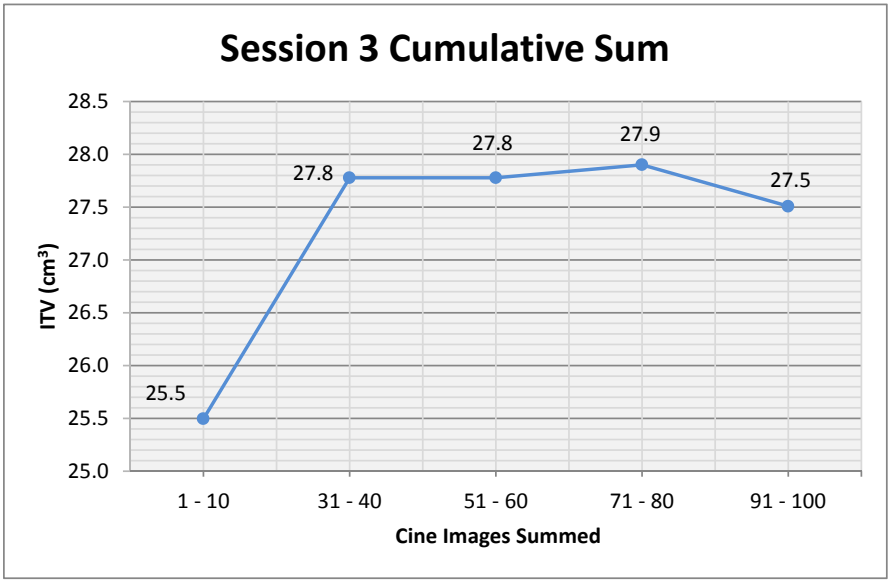

Figure 5.4: Intra-fractional changes in ITV value from Patient 7, using the images acquired in the third session of the cine images case: the cumulative sum was done by summing sets of ten images (starting with 1 to 10 until 91 to 100).

As shown in Figure 5.4, the ITV value varied 9% after summing 20 images. However,

this change gave an ITV value quite close to its final result. In this case, it could be said that not much new information was added to the tumour displacement description after the first 20 images. In addition, the decrease in the last images added suggests that after 50 images had been collected, the motion description only got reinforced. Since the number of images summed gave more weight to a certain motion trend (white area in the center of Figure 5.5), a smaller ITV value was obtained due to the 95% of the maximum voxel intensity threshold (step 5 in ITV segmentation procedure from cine images in section 4.3.3).

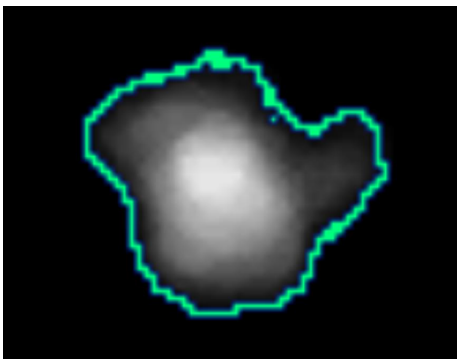

Figure 5.5: Axial view from the cumulative sum of 50 cine images from Patient 7 in the third session (grey scale area) and the final ITV result (green contour).

The same assessment can be done to verify the ITV result obtained from a 4DCT 10 phases data set cumulative sum. As shown in Figure 5.6, the result from the cumulative sum of the 10 phases seems to progressively add new information to the ITV's value. In addition, it can be seen that its ITV final value gives a closer result to the first and second session's final ITV value, than to the third session from Patient 7.

This last graphic from Figure 5.6 and ITV end result, seem to indicate that a 4DCT single session scan can be quite good in a session description where the breathing does not show drastic changes in the breathing amplitude, and possibly in the frequency, like in the case of patient 7 for the first and second session. But it might fail to account for the inter-fractional variation effects if there is a high intra-fractional tumour motion variation in one of the session (third session case).

It also seems reasonable to say that the 50 images used for the cine images case were enough to capture the breathing trace's variable pattern and that the same assessment to the 10 images in the 4DCT case showed a gradual increase in the ITV. Even so, since the 4DCT case was reconstructed according to phase, for each phase information that is added, the cumulative volume should increase, which supports our results. Nevertheless, further addition in the number of phases used might still measure a limited motion trend during the time used for each image reconstruction in the 4DCT data set.

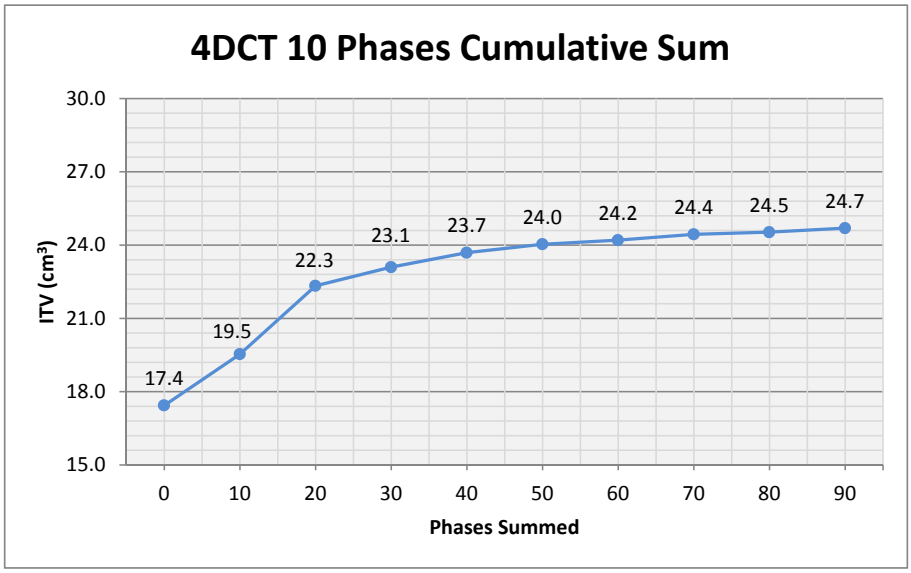

Figure 5.6: Intra-fractional changes in the ITV's value for the 10 phases 4DCT cumulative sum, from method 1, of Patient 7.

Chapter 6

General Conclusions

6.1 Thesis Conclusions

This work established a novel approach to validate the target motion estimate from a 4DCT scan in lung cancer radiotherapy. Based on image registration techniques and segmentation procedures, ITVs from 4DCT scans of 5 different patients were obtained and compared with the ITVs obtained through the same procedure in 3DCT axial cine mode images acquired in a random sequence over time.

From the first topic presented (section 5.1), it seemed that the comparison between ITVs in Table 5.2 suggested that 4DCT scans underestimated the ITV in an inter-fractional analysis, while the comparison in Table 5.4 gave the idea that the 4DCT ability to cope with intra-fractional changes was good. Therefore, based on the first observation, we would expect a risk of underdosing the tumour during the course of the radiotherapy, whereas from the second remark one 4DCT scan seems to be sufficient to estimate the intra-fractional tumour motion. This means that an adjustment for baseline shift prior to each treatment fraction could help to get a treatment delivery very close to the treatment plan, while considering the tumour motion in that fraction.

However, intra-fractional tumour motion is still ultimately dependent on breathing amplitude and in some cases, like Patient 7, the ITV changed from session to session, giving a cine images ITV bigger than the expected from the 4DCT case, which supports the result from the first Wilcoxon test present in Table 5.2. In other words, 4DCT ITV seems to be underestimated in an inter-fractional analysis.

In addition, when the same patient's 4DCT ITV was used in the intra-fractional analysis to be compared to different sessions' ITVs, it could be observed that the former conclusion taken through Table 5.4 did not seem to hold due to the highly variable breathing changes between treatment sessions in Patient 7.

Nevertheless, the approached used in section 5.2, to investigate the conclusions obtained from the Wilcoxon tests in section 5.1, only used a particular case of work (only one patient was seen in detail). Therefore, further analysis would be needed to be able to prove that the general conclusion from the second Wilcoxon test in Table 5.4, i.e., that the 4DCT scans can cope with intra-fractional variations, is not true.

In conclusion, the present study showed that the ITV creation based on conventional treatment planning 4DCT suffers a risk of underestimating the treatment volume and, as a consequence, missing the target. However, by correcting baseline shifts prior to each treatment fraction, the risk reduces considerably. Still, as seen in this work, the breathing amplitude might change from session to session and this endangers the 4DCT ITV validity.

6.2 Work Limitations

The present study had two main limitations: amount of patient data analysed and time spent in image analysis. Both limitations were directly related with the algorithm implemented for the segmentation procedure.

In the first limitation case, patient data analysed was restricted due to the fact that to ensure good segmentation methods, the tumours examined could not be attached to the lung wall, as it made the process of defining the tumours' border harder from one set of images to another, or be very diffuse, since it would also made the borders differentiation from bronchioles and bronchi structures difficult. This problem could be circumvented in two ways: either by increasing the number of patients used and pre-selecting them according to the criteria proposed in the study (but taking that into account before starting the tumour's segmentation process), or by developing a more detailed segmentation program. However, the last option requires another investigation about how to define tumours' border when they are attached to the wall in order to maintain the volume extraction as steady as possible between the image set analysis from different sessions and even from different breathing phases (the lung wall changes its shape from a phase to another). Furthermore, a definition is needed to differentiate the tumour from bronchioles and bronchi structures based on their voxel intensity level in the image and between different images (from a research point of view).

Also, for the second limitation case and last one, the efficiency in image analysis could have been improved through two ways. By normalizing all the images from a particular patient, a similar image gray scale could have been used and the segmentation process improved, since there would be less time needed to change the thresholds that selected the tumour volume in each image. In addition, since the MICE program limits the flexibility in delineating the tumour, one can maybe develop a segmentation script in MATLAB, Python or C# to extract the tumour in a more sophisticated and faster manner with comparable results.

Generally speaking, more time for image analysis and more patients data would improve even more this study's outcome.

6.3 Future Directions

As simple volume assessment is the most commonly reported method of comparing radiotherapy volumes [61], this study followed that line. However, a progression could be to combine that simple volume measure with some assessment about the volume's shape. To achieve this, Dice's similarity coefficient (DSC) can be used. This coefficient is frequently used for geometrical comparison analysis of radiotherapy target volume delineation methods, like volumetric overlap calculations [61], [62]. Its use could then serve as a way to compare results with previous works in the literature. However, DSC value and the conclusions taken from it should be based on a study with more data in order to have a statistical meaning, together with an appropriate statistical test, which does not fulfil the present study conditions.

Another proposed work would be to, after conducting a bigger study analysis through the methodology used in this work and with the suggestions proposed in section 6.2, reassess 4DCT validity for the corresponding ITV created in irregular breathing patients that follow breathing instructions. If the breathing becomes more regular, then the 4DCT artefacts caused by irregular breathing will be reduced and thus, the ITV's margins will be more reliable, reducing the radiation dose given to the normal tissue, for instance. In other words, a better control in the breathing of the patient can outweigh the ITV's underestimation that this study found. And so, the use of audiovisual biofeedback, referred to as a solution [63]–[65], should be considered as the next step to assess the validity of 4DCT determined ITV. Yet, we realised that this demands another study to investigate best pedagogical method to give feedback to the patient so that they could follow the guidance as best as possible.

Bibliography

[1] H. H. Liu, P. Balter, T. Tutt, B. Choi, J. Zhang, C. Wang, and et al., "Assessing Respiration-Induced Tumor Motion and Internal Target Volume Using Four-Dimensional Computed Tomography for Radiotherapy of Lung Cancer", *International Journal of Radiation Oncology, Biology and Physics*, vol. 68, no. 2, pp. 531–540, 2007. DOI: 10.1016/j.ijrobp.2006.12.066.

[2] P. J. Keall, G. S. Mageras, J. M. Balter, R. S. Emery, K. M. Forster, S. B. Jiang, and et al., "The management of respiratory motion in radiation oncology report of AAPM Task Group 76.", *Medical Physics*, vol. 33, no. 10, pp. 3874–3900, 2006. DOI: 10.1118/1.2349696.

[3] A. J. Cole, G. G. Hanna, S Jain, and J. M. O. Sullivan, "Motion Management for Radical Radiotherapy in Non-small Cell Lung Cancer", *Clinical Oncology*, vol. 26, pp. 67–80, 2014, ISSN: 0936-6555. DOI: 10.1016/j.clon.2013.11.001.

[4] T. Pawlicki, D. J. Scanderbeg, and G. Starkschall, *Hendee's Radiation Therapy Physics*, 4th ed. John Wiley & Sons, Inc., 2016, ISBN: 9780470376515.

[5] The International Commission on Radiation Units and Measurements, "ICRU Report 83: Prescribing, Recording and Reporting Photon Beam Therapy Intensity-Modulated Radiation Therapy (IMRT)", *Journal of the International Commission on Radiation Units and Measurements*, vol. 10, no. 1, NP, 2016. DOI: 10.1093/jicru/10.1.Report83. [Online]. Available: http://jicru.oxfordjournals.org/lookup/doi/10.1093/jicru/ndq001.

[6] E Rietzel, T Pan, and G. T. Chen, "Four-dimensional computed tomography: image formation and clinical protocol", *Medical Physics*, vol. 32, no. 4, pp. 874–889, 2005, ISSN: 0094-2405. DOI: 10.1118/1.1869852.

[7] D. De Ruysscher, C. Faivre-Finn, U. Nestle, C. W. Hurkmans, C. Le Péchoux, A. Price, and S. Senan, "European organisation for research and treatment of cancer recommendations for planning and delivery of high-dose, high-precision radiotherapy for lung cancer", *Journal of Clinical Oncology*, vol. 28, no. 36, pp. 5301–5310, 2010. DOI: 10.1200/JCO.2010.30.3271.

[8] A. P. Shah, P. A. Kupelian, B. J. Waghorn, T. R. Willoughby, J. M. Rineer, and et al., "Real-time tumor tracking in the lung using an electromagnetic tracking system", *International Journal of Radiation Oncology, Biology and Physics*, vol. 86, no. 3, pp. 477–483, 2013. DOI: 10.1016/j.ijrobp.2012.12.030.

[9] J. Sarker, A. Chu, K. Mui, J. A. Wolfgang, A. E. Hirsch, G. T. Y. Chen, and G. C. Sharp, "Variations in tumor size and position due to irregular breathing in 4D-CT: a simulation study.", *Medical Physics*, vol. 37, no. 3, pp. 1254–1260, 2010. DOI: 10.1118/1.3298007.

[10] N. Clements, T. Kron, R. Franich, L. Dunn, P. Roxby, Y. Aarons, B. Chesson, S. Siva, D. Duplan, and D. Ball, "The effect of irregular breathing patterns on internal target volumes in four-dimensional CT and cone-beam CT images in the context of stereotactic lung radiotherapy.", *Medical Physics*, vol. 40, no. 2, 021 904–n/a, 2013, ISSN: 2473-4209. DOI: 10.1118/1.4773310.

[11] B. W. Stewart and C. P. Wild, Eds., *World cancer report 2014*. International Agency for Research on Cancer, 2014, ISBN: 9789283204435.

[12] H. O. Kilgoz, G. Bender, J. M. Scandura, A. Viale, and B. Taneri, "KRAS and the Reality of Personalized Medicine in Non-Small Cell Lung Cancer", *Molecular Medicine*, vol. 22, pp. 380–387, 2016. DOI: 10.2119/molmed.2016.00151.

[13] B. Piperdi, A. Merla, and R. Perez-Soler, "Targeting angiogenesis in squamous non-small cell lung cancer", *Drugs*, vol. 74, no. 4, pp. 403–413, 2014, ISSN: 1179-1950. DOI: 10.1007/s40265-014-0182-z.

[14] A Hutchinson and P Bridge, "4DCT radiotherapy for NSCLC: a review of planning methods.", *Journal of Radiotherapy in Practice*, vol. 14, no. 1, pp. 70–79, 2015, ISSN: 1460-3969. DOI: 10.1017/S1460396914000041.

[15] O. Baykara, "Current Therapies and Latest Developments in Cancer Treatment", in *Horizons in Cancer Research*, H. S. Watanabe, Ed., vol. 57, Nova Science Publishers, Inc., 2015, ch. 8, pp. 105–156, ISBN: 978-1-63482-498-9.

[16] B. Reitz, D. S. Parda, A. Colonias, V. Lee, and M. Miften, "Investigation of Simple IMRT Delivery Techniques for Non-Small Cell Lung Cancer Patients with Respiratory Motion using 4DCT", *Medical Dosimetry*, vol. 34, no. 2, pp. 158–169, 2009. DOI: 10.1016/j.meddos.2008.07.001.

[17] J. E. Turner, *Atoms, Radiation, and Radiation Protection*, 3rd ed. Wiley-VCH Verlag GmbH & Co. KGaA, Weinheim, 2007, ISBN: 9783527406067. DOI: 10.1002/9783527616978.

[18] A. Maciejczyk, I. Skrzypczy, and M. Janiszewska, "Lung cancer. Radiotherapy in lung cancer: Actual methods and future trends", *Reports of practical oncology and radiotherapy*, vol. 19, pp. 353–360, 2014. DOI: 10.1016/j.rpor.2014.04.012.

[19] M. Guckenberger, N. Andratschke, H. Alheit, R. Holy, C. Moustakis, U. Nestle, and O. Sauer, "Definition of stereotactic body radiotherapy", *Strahlentherapie und Onkologie*, vol. 190, no. 1, pp. 26–33, 2014, ISSN: 1439-099X. DOI: 10.1007/s00066-013-0450-y.

[20] International Atomic Energy Agency, *The Role of PET/CT in Radiation Treatment Planning for Cancer Patient Treatment*. Vienna: International Atomic Energy Agency, 2008, IAEA-TECDOC-1603. [Online]. Available: http://www-pub.iaea.org/books/IAEABooks/8016/The-Role-of-PET-CT-in-Radiation-Treatment-Planning-for-Cancer-Patient-Treatment.

[21] N. B. Smith and A. Webb, *Introduction to Medical Imaging: Physics, Engineering and Clinical Applications*, ser. Cambridge Texts in Biomedical Engineering. Cambridge University Press, 2010, ISBN: 9780521190657.

[22] J. Ehrhardt and C. Lorenz, Eds., *4D Modeling and Estimation of Respiratory Motion for Radiation Therapy*, 1st ed. Springer-Verlag Berlin Heidelberg, 2013, pp. XX–341, ISBN: 9783642364402. DOI: 10.1007/978-3-642-36441-9.

[23] R. W. M. Underberg, F. J. Lagerwaard, J. P. Cuijpers, B. J. Slotman, J. R. S. Koste, and S Senan, "Four-Dimensional CT scans for treatment planning in stereotactic radiotherapy for stage I lung cancer", *International Journal of Radiation Oncology, Biology and Physics*, vol. 60, no. 4, pp. 1283–1290, 2004. DOI: 10.1016/j.ijrobp.2004.07.665.

[24] *Respiratory motion management for ct*, [Accessed 02-October-2017], 2013. [Online]. Available: http://clinical.netforum.healthcare.philips.com/global/Explore/White-Papers/CT/Respiratory-motion-management-for-CT.

[25] T. Pan, "Comparison of helical and cine acquisitions for 4D-CT imaging with multislice CT", *Medical Physics*, vol. 32, no. July 2004, pp. 627–634, 2005. DOI: 10.1118/1.1855013.

[26] J. D. Cox, J. Y. Chang, and R. Komaki, *Image-Guided Radiotherapy of Lung Cancer*. Informa Healthcare USA, Inc., 2008, ISBN: 9780849387838.

[27] J. W. H. Wolthaus, J.-J. Sonke, M. van Herk, J. S. a. Belderbos, M. M. G. Rossi, J. V. Lebesque, and E. M. F. Damen, "Comparison of different strategies to use four-dimensional computed tomography in treatment planning for lung cancer patients.", *International Journal of Radiation Oncology, Biology and Physics*, vol. 70, no. 4, pp. 1229–1238, 2008. DOI: 10.1016/j.ijrobp.2007.11.042.

[28] M. Ezhil, S. Vedam, P. Balter, B. Choi, D. Mirkovic, G. Starkschall, and J. Y. Chang, "Determination of patient-specific internal gross tumor volumes for lung cancer using four-dimensional computed tomography.", *Radiation Oncology*, vol. 4, no. 4, pp. 1–14, 2009. DOI: 10.1186/1748-717X-4-4.

[29] T. Yamamoto, U. Langner, B. W. Loo, J. Shen, and P. J. Keall, "Retrospective Analysis of Artifacts in Four-Dimensional CT Images of 50 Abdominal and Thoracic Radiotherapy Patients", *International Journal of Radiation Oncology, Biology and Physics*, vol. 72, no. 4, pp. 1250–1258, 2008. DOI: 10.1016/j.ijrobp.2008.06.1937.

[30] D. Han, J. Bayouth, and S. Bhatia, "Characterization and identification of spatial artifacts during 4D-CT imaging", *Medical Physics*, vol. 38, no. 4, pp. 2074–2087, 2011. DOI: 10.1118/1.3553556.

[31] J. D. Ruben, A Seeley, V Panettieri, and T Ackerly, "Variation in Lung Tumour Breathing Motion between Planning Four-dimensional Computed Tomography and Stereotactic Ablative Radiotherapy Delivery and its Dosimetric Implications : Any Role for Four-dimensional Set-up Verification?", *Clinical Oncology*, vol. 28, pp. 21–27, 2016. DOI: 10.1016/j.clon.2015.08.010.

[32] H.-U. Kauczor and C. Plathow, "Imaging tumour motion for radiotherapy planning using MRI", *Cancer Imaging*, vol. 6, no. October, pp. 140–144, 2006. DOI: 10.1102/1470-7330.2006.9027.

[33] R. Muirhead, S. G. McNee, C. Featherstone, K. Moore, and S. Muscat, "Use of Maximum Intensity Projections (MIPs) for target outlining in 4DCT radiotherapy planning.", *Journal of Thoracic Oncology*, vol. 3, no. 12, pp. 1433–1438, 2008. DOI: 10.1097/JTO.0b013e31818e5db7.

[34] R. W. M. Underberg, F. J. Lagerwaard, B. J. Slotman, J. P. Cuijpers, and S. Senan, "Use of Maximum Intensity Projection (MIP) for Target Volume Generation in 4DCT Scans for Lung Cancer", *International Journal of Radiation Oncology, Biology and Physics*, vol. 63, no. 1, pp. 253–260, 2005. DOI: 10.1016/j.ijrobp.2005.05.045.

[35] Y. Seppenwoolde, H. Shirato, K. Kitamura, S. Shimizu, M. V. Herk, J. V. Lebesque, and K. Miyasaka, "Precise and Real-Time Measurement of 3D Tumor Motion in Lung due to Breathing and Heartbeat, Measured During Radiotherapy", *International Journal of Radiation Oncology, Biology and Physics*, vol. 53, no. 4, pp. 822–834, 2002. DOI: 10.1016/S0360-3016(02)02803-1.

[36] Y. Wang, Y. Bao, L. Zhang, W. Fan, H. He, Z.-w. Sun, X. Hu, S.-m. Huang, M. Chen, and X.-w. Deng, "Assessment of Respiration-Induced Motion and Its Impact on Treatment Outcome for Lung Cancer", *BioMed Research International*, vol. 2013, pp. 1–10, 2013. DOI: 10.1155/2013/872739.

[37] K. R. Britton, G. Starkschall, S. L. Tucker, T. Pan, C. Nelson, J. Chang, J. D. Cox, R. Mohan, and R. Komaki, "Assessment of Gross Tumor Volume Regression and Motion Changes During Radiotherapy for Non Small-Cell Lung Cancer as Measured by Four-Diomensional Computed Tomography", *International Journal of Radiation Oncology, Biology and Physics*, vol. 68, no. 4, pp. 1036–1046, 2007. DOI: 10.1016/j.ijrobp.2007.01.021.

[38] T. Bai, J. Zhu, Y. Yin, J. Lu, H. Shu, L. Wang, and B. Yang, "How does four-dimensional computed tomography spare normal tissues in non-small cell lung cancer radiotherapy by defining internal target volume?", *Thoracic Cancer*, vol. 5, no. 6, pp. 537–542, 2014. DOI: 10.1111/1759-7714.12126.

[39] E. Rietzel, A. K. Liu, K. P. Doppke, J. A. Wolfgang, A. B. Chen, G. T. Y. Chen, and N. C. Choi, "Design of 4D treatment planning target volumes", *International Journal of Radiation Oncology, Biology and Physics*, vol. 66, no. 1, pp. 287–295, 2006. DOI: 10.1016/j.ijrobp.2006.05.024.

[40] S. S. James, P. Mishra, F. Hacker, R. I. Berbeco, and J. H. Lewis, "Quantifying ITV instabilities arising from 4DCT: A simulation study using patient data", *Physics in Medicine and Biology*, vol. 57, no. 5, pp. L1–L7, 2012. DOI: 10.1088/0031-9155/57/5/L1.

[41] F. X. Li, J. B. Li, Y. J. Zhang, T. H. Liu, S. Y. Tian, M. Xu, D. P. Shang, and C. S. Ma, "Comparison of the planning target volume based on three-dimensional CT and four-dimensional CT images of non-small-cell lung cancer", *Radiotherapy and Oncology*, vol. 99, no. 2, pp. 176–180, 2011. DOI: 10.1016/j.radonc.2011.03.015.

[42] F. Li, J. Li, Z. Ma, Y. Zhang, J. Xing, H. Qi, and D. Shang, "Comparison of internal target volumes defined on 3-dimensional, 4-dimensonal, and cone-beam CT images of non-small-cell lung cancer", *OncoTargets and Therapy*, vol. 9, pp. 6945–6951, 2016. DOI: 10.2147/OTT.S111198.

[43] K. Harada, N. Katoh, R. Suzuki, Y. M. Ito, and S. Shimizu, "Evaluation of the motion of lung tumors during stereotactic body radiation therapy (SBRT) with four-dimensional computed tomography (4DCT) using real-time tumor-tracking radiotherapy system (RTRT)", *Physica Medica*, vol. 32, pp. 305–311, 2016. DOI: 10.1016/j.ejmp.2015.10.093.

[44] J. Cai, P. W. Read, J. M. Baisden, J. M. Larner, S. H. Benedict, and K. Sheng, "Estimation of Error in Maximal Intensity Projection-Based Internal Target Volume of Lung Tumors: A Simulation and Comparison Study Using Dynamic Magnetic Resonance Imaging", *International Journal of Radiation Oncology, Biology and Physics*, vol. 69, no. 3, pp. 895–902, 2007. DOI: 10.1016/j.ijrobp.2007.07.2322.

[45] H. Ge, J. Cai, C. R. Kelsey, and F.-F. Yin, "Quantification and minimization of uncertainties of internal target volume for stereotactic body radiation therapy of lung cancer.", *International Journal of Radiation Oncology, Biology and Physics*, vol. 85, no. 2, pp. 438–443, 2013. DOI: 10.1016/j.ijrobp.2012.04.032.

[46] A. V. Louie, G. Rodrigues, J. Olsthoorn, D. Palma, E. Yu, B. Yaremko, B. Ahmad, I. Aivas, and S. Gaede, "Inter-observer and intra-observer reliability for lung cancer target volume delineation in the 4D-CT era", *Radiotherapy and Oncology*, vol. 95, no. 2, pp. 166–171, 2010, ISSN: 0167-8140. DOI: 10.1016/j.radonc.2009.12.028.

[47] D. J. H. Joseph V. Hajnal Derek L.G. Hill, *Medical Image Registration*, M. Neuman, Ed. CRC Press, Inc., 2001, ISBN: 0849300649.

[48] C. Thilmann, S. Nill, T. Tücking, A. Höss, B. Hesse, L. Dietrich, R. Bendl, B. Rhein, P. Häring, C. Thieke, U. Oelfke, J. Debus, and P. Huber, "Correction of patient positioning errors based on in-line cone beam CTs : clinical implementation and first experiences", *Radiation Oncology*, vol. 1, p. 16, 2006, ISSN: 1748-717X. DOI: 10.1186/1748-717X-1-16.

[49] R. C. Gonzalez and R. E. Woods, *Digital Image Processing*, 2nd ed. Prentice-Hall, Inc., 2002, ISBN: 0201180758.

[50] A. X. Falcão, J. K. Udupa, S. Samarasekera, S. Sharma, B. E. Hirsch, and R. de A. Lotufo, "User-Steered Image Segmentation Paradigms : Live Wire and Live Lane", *Graphical Models and Image Processing*, vol. 60, no. 4, pp. 233–260, 1998. DOI: https://doi.org/10.1006/gmip.1998.0475.

[51] J. M.R. S. Tavares and R. M. N. Jorge, *Computational Vision and Medical Image Processing V: Proceedings of the 5th Eccomas Thematic Conference on Computational Vision and Medical Image Processing (VipIMAGE2015, Tenerife, Spain, October 19-21, 2015)*. CRC Press, Inc., 2015, ISBN: 9781138029262.

[52] P. Giraud, M. Antoine, A. Larrouy, B. Milleron, P. Callard, Y. D. Rycke, M.-F. Carette, J.-C. Rosenwald, J.-M. Cosset, M. Housset, and E. Touboul, "Evaluation of Microscopic Tumor Extension in Non-Small-Cell Lung Cancer for Three-Dimensional Conformal Radiotherapy Planning", *Physics in Medicine and Biology*, vol. 48, no. 4, pp. 1015–1024, 2000. DOI: http://dx.doi.org/10.1016/S0360-3016(00)00750-1.

[53] J. M. Kilburn, J. T. Lucas, M. H. Soike, D. N. Ayala-peacock, W Blackstock, W. H. Hinson, M. T. Munley, W. J. Petty, and J. J. Urbanic, "Is a Clinical Target Volume (CTV) Necessary in the Treatment of Lung Cancer in the Modern Era Combining 4-D Imaging and Image-guided Radiotherapy (IGRT)?", *Cureus*, vol. 8, no. 1, pp. 1–15, 2016. DOI: 10.7759/cureus.466.

[54] *Medical interactive creative environment*, [Accessed 14-July-2017]. [Online]. Available: http://gentleradiotherapy.se/downloads/mice/.

[55] F. E.-Z. A. El-gamal, M. Elmogy, and A. Atwan, "Current trends in medical image registration and fusion", *Egyptian Informatics Journal*, vol. 17, no. 1, pp. 99–124, 2016, ISSN: 1110-8665. DOI: 10.1016/j.eij.2015.09.002.

[56] S. Siegel, *Nonparametric statistics for the behavioral sciences*. McGraw-Hill Companies, 1956, ISBN: 0070573484.

[57] P. S. Mann, *Introdutory Statistics*, 7th ed., N. W. Hoboken, Ed. John Wiley & Sons, Inc., 2010, ISBN: 0470444665.

[58] M. L. M. Richard William Madsen, *Statistical Concepts: With Applications to Business and Economics*. Prentice-Hall, Inc., 1980, ISBN: 0138448787.

[59] T. Sincich, *Business Statistics by Example*, 3rd ed. Macmillan Publishing Company, 1990, ISBN: 002946126x.

[60] H. Shirato, Y. Seppenwoolde, K. Kitamura, R. Onimura, and S. Shimizu, "Intrafractional Tumor Motion: Lung and Liver", *Seminars in Radiation Oncology*, vol. 14, no. 1, pp. 10–18, 2004. DOI: 10.1053/j.semradonc.2003.10.008.

[61] G. G. Hanna, A. R. Hounsell, and J. M. O. Sullivan, "Geometrical Analysis of Radiotherapy Target Volume Delineation : a Systematic Review of Reported Comparison Methods Statement of Search Strategies Used and Sources of Information", *Clinical Oncology*, vol. 22, pp. 515–525, 2010. DOI: 10.1016/j.clon.2010.05.006.

[62] W. R. Crum, O. Camara, and D. L. G. Hill, "Generalized Overlap Measures for Evaluation and Validation in Medical Image Analysis", *IEEE Transactions on Medical Imaging*, vol. 25, no. 11, pp. 1451–1461, 2006. DOI: 10.1109/TMI.2006.880587.

[63] D. Lee, P. B. Greer, J. Ludbrook, J. Arm, P. Hunter, S. Pollock, and et al., "Audiovisual Biofeedback Improves Cine-Magnetic Resonance Imaging Measured Lung Tumor Motion Consistency", *International Journal of Radiation Oncology, Biology and Physics*, vol. 94, no. 3, pp. 628–636, 2016. DOI: 10.1016/j.ijrobp.2015.11.017.

[64] R. B. Venkat, A. Sawant, Y. Suh, R. George, and P. J. Keall, "Development and preliminary evaluation of a prototype audiovisual biofeedback device incorporating a patient-specific guiding waveform.", *Physics in Medicine and Biology*, vol. 53, no. 11, N197, 2008. DOI: 10.1088/0031-9155/53/11/N01.

[65] T. Neicu, R. Berbeco, J. Wolfgang, and S. B. Jiang, "Synchronized moving aperture radiation therapy (SMART): improvement of breathing pattern reproducibility using respiratory coaching.", *Physics in Medicine and Biology*, vol. 51, pp. 617–636, 2006. DOI: 10.1088/0031-9155/51/3/010.